Assessing the spatiotemporal dynamics of seasonal and perennial surface water resources across Lesotho's agroecological zones ☆

Article *in* International Journal of Applied Earth Observation and Geoinformation · July 2025

DOI: 10.1016/j.jag.2025.104688

CITATIONS
0

READS
45

4 authors, including:

Kunwar K. Singh
William & Mary
46 PUBLICATIONS **1,187** CITATIONS
SEE PROFILE

Ariel Benyishay
William & Mary
51 PUBLICATIONS **1,568** CITATIONS
SEE PROFILE

TŠepiso A. RantŠo
National University of Lesotho
18 PUBLICATIONS **109** CITATIONS
SEE PROFILE

International Journal of Applied Earth Observation and Geoinformation 142 (2025) 104688

Contents lists available at ScienceDirect

International Journal of Applied Earth Observation and Geoinformation

journal homepage: www.elsevier.com/locate/jag

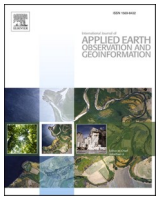

Assessing the spatiotemporal dynamics of seasonal and perennial surface water resources across Lesotho's agroecological zones☆

Kunwar K. Singh [a,*], Sayedeh Sara Sayedi [a], Ariel BenYishay [a], Tšepiso A. Rantšo [b]

[a] AidData, Global Research Institute, William & Mary, VA 23185, USA
[b] Department of Development Studies, National University of Lesotho, Roma, Lesotho

ARTICLE INFO

Keywords:
Sub-Saharan Africa
Seasonal and perennial water bodies
Spectral indices
Agroecological zones (AEZs)
Sentinel imagery
Random Forest algorithm
Surface water dynamics

ABSTRACT

Surface water resources are crucial for agricultural productivity and rural livelihoods, particularly in water-scarce regions such as Sub-Saharan Africa. In Lesotho, understanding the dynamics of seasonal and perennial water bodies is vital for informed water resource management and policy development. This study evaluates spectral indices for mapping and analyzing the spatiotemporal dynamics of surface water across different agroecological zones (AEZs) in Lesotho from 2016 to 2024 water years. Using harmonized Sentinel imagery integrated into a Random Forest machine-learning framework, we applied a range of water, vegetation, and soil indices to map surface water monthly and distinguish between seasonal and perennial water surfaces. Our findings reveal that the water ratio index was the most effective for mapping surface water across AEZs, outperforming others in distinguishing water from rangeland, cropland, and bare soil. Additional indices further improved water delineation in specific AEZs. Although no significant differences in classification accuracy were observed across AEZs ($p > 0.05$), visual inspection revealed misclassifications, mainly false positives, which could lead to overestimates of water area. Surface water trends vary regionally, with a significant increase in perennial water in the Foothills and Mountains, while seasonal water shows a non-significant decline, indicating divergent hydrological trajectories. These findings underscore the need for region-specific assessments and management strategies to address the evolving hydrological regimes. Our study provides a scalable framework for water resource assessment applicable beyond Lesotho, with significant implications for addressing water scarcity and guiding policies on water storage, climate-smart agriculture, and community-based governance in Sub-Saharan Africa.

1. Introduction

Seasonal variations in surface water availability—driven by agricultural demands, urban expansion, and erratic weather patterns exacerbated by global climate change—often lead to regional water scarcity, even in regions with overall abundant water resources. With agriculture accounting for nearly two-thirds of global water withdrawals (Grafton et al., 2018), sustainable water management is crucial, particularly in rainfed-dependent regions of Sub-Saharan Africa (Karpouzoglou and Barron, 2014; Kotir, 2011). In these regions, unpredictable water availability directly impacts agricultural productivity and, consequently, food security (Biazin et al., 2012). Sub-Saharan African countries, such as Lesotho, characterized by complex topography, dependence on rainfall and snowmelt, and diverse agroecological zones (AEZ), are especially vulnerable to these fluctuations (De Pauw et al., 2000). This underscores the need for effective monitoring strategies to optimize water resource utilization (Matarira et al., 2014). Time-series mapping using remotely sensed satellite imagery offers a robust approach for assessing inter- and intra-annual variations in surface water at broad scales. While global surface water databases exist (Thorslund and Van Vliet, 2020), country-specific mapping often requires customization to account for local conditions within AEZs, including topography and irrigation infrastructure (Herndon et al., 2020). This approach is especially valuable for Lesotho, where hydrological monitoring networks exist but remain limited in coverage, highlighting the need for expanded monitoring to support

☆ This article is part of a special issue entitled: 'African EO – Mapping – Invited' published in International Journal of Applied Earth Observation and Geoinformation.

* Corresponding author.
E-mail address: ksingh@aiddata.wm.edu (K.K. Singh).

https://doi.org/10.1016/j.jag.2025.104688
Received 23 October 2024; Received in revised form 3 June 2025; Accepted 17 June 2025

comprehensive water resource management. Prioritizing the accurate mapping of seasonal (e.g., ephemeral streams or ponds) and perennial (i.e., maintain a continuous presence of water throughout the year) surface water bodies is therefore critical for understanding inter- and intra-annual variation to inform evidence-based water resource allocation in regions prone to water scarcity for enhancing the resilience of vulnerable agricultural systems.

Advancements in remote sensing technology, coupled with freely available satellite imagery from platforms such as Landsat, Sentinel, and MODIS, have significantly enhanced our capacity to monitor surface water dynamics (Sheffield et al., 2018). These satellite systems offer high temporal and spatial resolutions, enabling the detection of both seasonal and perennial water bodies. Spectral water indices have become a reliable and efficient means for identifying surface water, particularly in large regions with diverse topographies where traditional methods are less feasible (Sagan et al., 2020). Among the most widely adopted indices are the normalized difference water index (NDWI), modified normalized difference water index (MNDWI), and automated water extraction index (AWEI), each leveraging the distinct spectral reflectance properties of water (Guo et al., 2017; Lu et al., 2011; Zhou et al., 2017). The NDWI, introduced by McFEETERS (1996), remains a widely adopted index for water mapping by distinguishing water from other cover types using green and near-infrared (NIR) bands. However, its accuracy diminishes in complex terrain or dense vegetation, where spectral interference reduces detection reliability (Guo et al., 2017). To overcome these limitations, variations like the MNDWI, which incorporates shortwave infrared (SWIR) instead of NIR, have been developed to improve water detection in urban and arid landscapes (Xu, 2006). Similarly, the AWEI (Feyisa et al., 2014) enhances water identification in environments with high spectral reflectance variability, such as urban or mountainous regions. While effective for mapping larger, perennial water bodies, these indices struggle to detect transient water resources that fluctuate seasonally in response to rainfall. Conventional indices, designed for stable, perennial water features, often overlook these short-lived seasonal water bodies (Campos et al., 2012). In addition, accurately capturing their spatiotemporal extent and variability requires sophisticated time-series analysis, as single satellite imagery is insufficient for characterizing such dynamic systems (Haas et al., 2009). This limitation highlights the need for customized methodologies that leverage the temporal dimension of satellite data to improve surface water resource mapping.

Detecting seasonal water bodies in topographically complex and ecologically diverse regions presents considerable challenges due to shadows, elevation-induced reflectance variations, and spectral interference from vegetation, all of which hinder the extraction of water features from satellite imagery (Soti et al., 2009). The inherent inconsistencies in these environmental factors can compromise the accuracy of even the most sophisticated water indices in capturing dynamic surface water bodies. The ephemeral nature of perennial water bodies, characterized by their small size and transient existence tied to rainfall patterns, necessitates the development of methodological frameworks capable of accounting for temporal fluctuations in water availability and concurrent changes in landscape characteristics (Soti et al., 2009). Integrating multi-source data—such as vegetation indices, soil moisture indices, and topographic measures—can significantly improve the detection of perennial water bodies. For instance, studies have demonstrated the effectiveness of Landsat imagery with NDWI variants in enhancing the mapping of perennial surface waters, particularly in areas like the Sahara-Sahel transition zone (Campos et al., 2012). Furthermore, modifications to existing indices, such as substituting the green band with the mid-NIR band in NDWI, can improve water detection in sparsely vegetated areas. This highlights the importance of region-specific adaptations to minimize interference from surrounding land cover and optimize water detection accuracy. Comparative studies have shown that the performance of various water indices is context-dependent, emphasizing the need for careful selection and customization based on local geographic and environmental conditions. Acharya et al. (2019) and Zhou et al. (2017) highlight that the effectiveness of water index varies with terrain and vegetation cover characteristics. Moreover, factors such as snow cover and soil moisture can impact the accuracy of indices like the AWEI and water ratio index (WRI) (Khalid et al., 2021). Therefore, tailored methodologies are essential for accurately monitoring regions with high spatiotemporal variability in water resources, ensuring reliable assessments of water availability.

In regions with complex terrain or heterogeneous land cover, machine learning techniques provide a robust and increasingly effective alternative for improving water detection accuracy (Bangira et al., 2019; Bentivoglio et al., 2022; Sit et al., 2020). Machine learning algorithms, such as Random Forest (RF) and support vector machines, excel at integrating diverse data sources and accounting for spectral reflectance variability (Pal and Mather, 2005), thus overcoming limitations inherent in traditional threshold-based methods. Their advanced classification capabilities enable robust differentiation of water bodies from other land cover types, even in challenging landscapes. The strength of machine learning lies in its ability to incorporate a wide range of data, including time series vegetation indices and topographic measures, facilitating a comprehensive approach to water classification (Maxwell et al., 2018). For instance, integrating multiple water indices and topographic data in RF models can effectively address spectral complexities introduced by diverse landforms and cover types, substantially improving classification accuracy (Chen et al., 2020). However, while the RF algorithm is effective for classification and regression, it can struggle with temporal dependencies, a limitation addressed by incorporating time-sensitive variables, structuring the dataset with multi-year rolling averages and annual composites, and employing a temporally aware cross-validation strategy. The strategic application of machine learning represents a transformative advancement in detecting both seasonal and perennial water bodies in regions with complex terrain and dynamic water availability patterns. This is particularly relevant in areas where conventional methods are challenged by steep topography, varied land cover, and seasonal fluctuations (Pryor et al., 2022). Investing in and implementing these advanced techniques is paramount for ensuring water security and environmental stewardship in vulnerable areas.

Lesotho serves as an ideal case study for evaluating spectral indices in characterizing seasonal and perennial surface water resources and analyzing their spatiotemporal dynamics across diverse AEZs. We applied a range of water, vegetation, and soil spectral indices derived from Sentinel imagery within a RF machine-learning framework to map surface water at a monthly interval from October 2015 to September 2024. Through this effort, we identified the most effective index combinations for accurately detecting water bodies within each AEZ and subsequently categorized the mapped water cover into seasonal and perennial surfaces. A key novelty of this approach lies in distinguishing seasonal from perennial surface waters, enabling the capture of critical spatiotemporal fluctuations in surface water availability. We assessed interannual variability to understand long-term changes, and intra-annual variability to highlight seasonal water dynamics. These insights inform targeted water mapping strategies for Lesotho and similar regions in Sub-Saharan Africa, where understanding spatiotemporal surface water dynamics is crucial for sustaining agricultural productivity and rural livelihoods. The ability to monitor water availability through remote sensing has significant policy implications, particularly in regions facing increasing water scarcity. Data-driven policies could support investments in water storage infrastructure, modern irrigation techniques, climate-smart agriculture, community-based water governance, and regional cooperation on water resources.

2. Material and methods

2.1. Study area

Lesotho, a landlocked country covering 30,355 Km^2 within South Africa, is situated at the convergence of the Maluti and Drakensberg Mountain ranges (Fig. 1). It comprises four AEZs—Lowlands, Foothills, Highlands (hereafter referred to as Mountains), and the Senqu River Valley (SRV)—each with distinct hydrological and land-use attributes (Fig. S1; Table S1). Elevation ranges from approximately 3,500 m at its highest points to around 1,500 m at the confluence of the Orange and Makhaleng rivers (Ramakhanna et al., 2022). Known as the "water tower" of Southern Africa, Lesotho plays a key role in regional water supply. The Lesotho Highlands Water Project delivers water to South Africa (Hoag, 2019; Keketso, 2003; Mwangi, 2007), while the Lowlands Water Project supplies urban centers such as Roma, Morija, and Teyateyaneng from the Metolong dam on the Phuthiatsana River (Sekamane et al., 2023). Despite its abundant water resources, growing urban water demands have placed stress on the agricultural sector, especially in rural regions reliant on seasonal rainfall.

Climate change in recent years has intensified water scarcity challenges for agriculture. The El Niño-induced drought of 2012–2014, for example, caused substantial reductions in agricultural output among smallholder farmers (Hlalele, 2017). Precipitation patterns in Lesotho exhibit significant variability due to its diverse topography (Sene et al., 1998), with the northeastern Mountains receiving up to 1,600 mm of rainfall annually, while the rain-shadowed SRV records only 300–500 mm due to orographic effects (Moeletsi and Walker, 2012; Nash and Grab, 2010). Approximately 85 % of the country's precipitation occurs between October and April, peaking during the summer months from December to February (Sene et al., 1998). Snowfall is also prevalent in high-altitude areas, particularly in the northeastern Mountains, affecting local water availability. Temperature patterns further reflect this topographic diversity: average minimum temperatures in winter (May to July) reach −6.3 °C in the Mountains, compared to 5.1 °C in the lowlands, while maximum temperatures in summer (November to February) average 16.5 °C in the Mountains and 29 °C in the Lowlands (Moeletsi and Walker, 2012).

Despite Lesotho's abundant surface water resources, agricultural productivity remains highly vulnerable to water variability due to a heavy reliance on rainfall and limited irrigation infrastructure, with only 1.2 % of cultivated land being irrigated (Verschuur et al., 2021). This heavy reliance on rainfall, compounded by climate change, presents significant challenges for water resource management and agricultural resilience. Land degradation further compounds these issues. Soil erosion has reduced arable land from 13 % to 9 %, severely impacting farming capacity (Love, 1996). Unsustainable land use practices also contribute to land degradation across AEZs (https://renoka.org), with specific manifestations including grassland degradation in high-altitude regions linked to overgrazing, woody vegetation encroachment in mid-altitude zones, and agricultural expansion in lower elevations driven by population growth (Mbata, 2001). While both overgrazing and climate change contribute to land degradation, evidence suggests that overgrazing may be the more immediate and dominant driver in certain contexts (Turpie et al., 2021). The northern Lowlands and Foothills, home to 80 % of the population, face severe land degradation and heightened climate vulnerabilities, directly impacting food security and water availability. In contrast, the Mountains AEZ, which covers 59 % of the country, primarily supports livestock farming, as its short growing seasons limit crop cultivation. Moreover, large-scale dam projects, while aimed at improving water security, pose socio-economic risks, including displacement of highland communities and the reduction of arable land. Addressing these interrelated climatic, hydrological, and land-use challenges necessitates enhanced water management strategies, particularly for subsistence farmers who depend on seasonal water variability (Gwimbi and Rakuoane, 2019). Strengthening monitoring systems, promoting sustainable land-use practices, and enhancing irrigation efficiency will be critical for improving agricultural resilience and

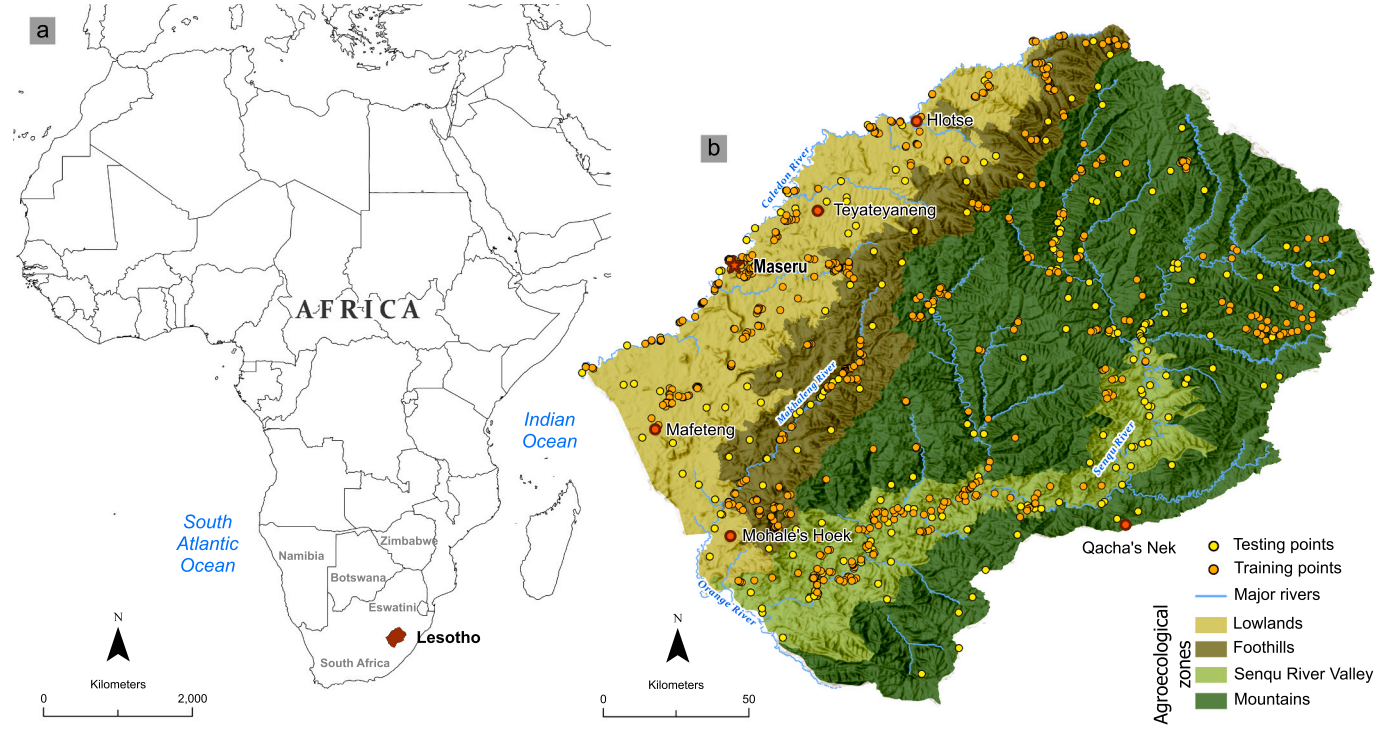

Fig. 1. The map illustrates Lesotho's four agroecological zones—Foothills, Lowlands, Mountains, and Senqu River Valley—overlaid on a high-resolution topographical relief map. This representation highlights the country's diverse elevation and terrain features that shape its agroecological characteristics. Major river systems are shown in blue, while yellow and white points indicate the locations of training and testing data, respectively. (For interpretation of the references to colour in this figure legend, the reader is referred to the web version of this article.)

securing livelihoods in the face of ongoing environmental changes.

2.2. Ground observations data acquisition

2.2.1. Ground surveys

To enhance the accuracy and reliability of our study, we engaged local experts to conduct field surveys over two consecutive growing seasons from 2021 to 2023. This collaboration facilitated the collection of *in-situ* observational data encompassing seasonal and perennial water bodies and irrigation infrastructures prevalent in the region, including a range of crop types. The experts surveyed several surface water bodies, including the Mohokare River, the Phuthiatsana River, and several small reservoirs utilized for irrigation purposes within the Lowlands AEZ. Surveyors documented spatial coordinates (i.e., longitude and latitude) of water bodies and cataloged irrigation infrastructures, encompassing furrow irrigation, drip irrigation systems, and traditional methods such as river diversions. A total of 117 surface water bodies were identified within the Lowlands AEZ.

Surface water resources were further categorized into seasonal and perennial based on input from local smallholder farmers and verified through visual interpretation of remotely sensed imagery. Seasonal water bodies were identified by their intermittent surface water presence, capturing phenomena such as seasonal flooding, ephemeral river flows during the wet season, and irrigation practices dependent on rainfall patterns. Conversely, perennial water bodies, such as rivers, stone dams, wetlands, and reservoirs, maintained a continuous presence of water throughout the study period. This categorization enhances understanding of the hydrological dynamics of the region by distinguishing stable water sources from fluctuating ones.

We subsequently combined ground observations from field surveys with visual interpretation techniques to collect seasonal and perennial water bodies reference data for other AEZs for classification from online remote sensing databases (e.g., Google Earth Pro, ESRI basemaps). During the visual interpretation, in instances where cloud cover obscured imagery during the rainy season, we inferred the presence of water in both seasonal and perennial water bodies. This inference was based on the expected hydrological conditions during that period, which helped us characterize and quantify water bodies across AEZs.

2.2.2. Visual interpretation of very high-resolution satellite imagery

We utilized very high-resolution imagery archived in Google Earth Pro and ESRI basemaps to identify and collect reference observation data through visual interpretation techniques and later verified using the Global Surface Water Dataset from the Joint Research Center Data Catalogue (https://data.jrc.ec.europa.eu) for accurate surface water mapping (Liang et al., 2018). These data were supplemented with *in-situ* observations. The visual interpretation of satellite imagery from 2004 to 2024 across the AEZs yielded 728-point locations that were used for training classification models (Fig. 1).

Instead of partitioning the dataset into training and testing subsets, as is common in machine-learning-based land use and land cover mapping, we acquired a separate testing dataset of 254-point locations for validating the classification models (Fig. 1). This was accomplished by creating random points using the WorldCover 2021 dataset (Zanaga et al., 2022) and correcting any mislabeled points through visual inspection of the archived high-resolution imagery from Google Earth Pro and Landsat 8 imagery for 2013, resulting in a final testing dataset of 254 points. This approach ensured a spatially representative distribution of training points while preserving the integrity of the testing dataset, thereby enhancing model robustness and facilitating more accurate comparative analyses. This methodology mitigates the inherent limitations of random data partitioning in RF models by providing explicit control over the training data composition—a critical consideration for analyzing water bodies, which typically constitute a small proportion of the overall land cover. This systematic sampling approach involved selecting representative sample points within AEZs with known water resources, specifically targeting larger bodies such as rivers and wetlands. Strategic placement of observations on or near these water sources established robust reference points for both unambiguous surface water features and identifiable non-water features, including areas subject to seasonal flooding (Table 1).

2.3. Remote sensing data acquisition and processing

Selecting satellite imagery for mapping of water bodies requires careful consideration of their spatial and temporal resolutions to optimize the balance between detection accuracy and historical continuity. While imagery from Landsat and Moderate Resolution Imaging Spectroradiometer (MODIS) sensors are frequently employed for surface water analysis across different scales, their relatively coarse spatial resolution constrains their capacity to detect smaller water bodies, such as narrow tributaries, small reservoirs, and seasonal wetlands (Feyisa et al., 2014; Li et al., 2021). For instance, Landsat imagery, with its 30-meter resolution and 16-day revisit cycle, offers an unparalleled historical record dating back to the 1970 s, making it ideal for long-term environmental monitoring. However, its spatial resolution is insufficient for accurately delineating the network of small tributaries and reservoirs, specifically those located in Mountains AEZ (Bhagat and Sonawane, 2011; Mueller et al., 2016).

To overcome these limitations, we selected Sentinel-2 imagery, favoring it over synthetic aperture radar (SAR) and coarser optical datasets. The MultiSpectral Instrument (MSI) onboard Sentinel sensor offers superior spatial resolution (up to 10 m), which facilitates improved mapping of narrow rivers and small reservoirs. SAR-based indices were deemed unsuitable due to the considerable computational resources required for preprocessing steps (e.g., speckle filtering and terrain correction) and the complications arising from Lesotho's rugged topography. The rugged terrain induces geometric distortions like layover and shadow effects, which can misrepresent water body extent, especially in steep valleys and gorges. Furthermore, SAR encounters difficulties in distinguishing open water from wetlands or irrigated fields, potentially leading to classification errors. Automatic backscatter thresholding is effective for mapping unvegetated surface water but requires region-specific adaptation, posing challenges in diverse landscapes. Seasonal variations and surface roughness further complicate accurate water detection, as increased backscatter can cause flowing water to be misidentified as land (Amitrano et al., 2024).

To maximize spatial and temporal resolution, we utilized the Harmonized Sentinel-2 MSI, Level-1C (TOA - top-of-atmosphere reflectance) dataset. Harmonized Sentinel-2 MSI data are processed to ensure consistency with other satellite datasets, particularly Landsat. Uniform processing steps—such as atmospheric correction and radiometric calibration—are applied to produce a seamless, globally consistent dataset on a common scale. This harmonization enables consistent surface

Table 1
Ground observation data, comprising both water and non-water surfaces (e.g., forest, farmlands, and other land covers), were collected using visual interpretation techniques and *in-situ* surveys. This data was used to quantify surface water extent and assess its dynamics. The Foothills AEZ has the fewest water samples due to the infrequent surface water occurrence in the zone.

Agroecological zones (AEZs)	Training data			Testing data		
	Surface water bodies	Other land cover types	Total	Surface water bodies	Other land cover types	Total
Lowlands	135	151	286	21	25	46
Foothills	37	134	171	26	25	51
Mountains	55	89	144	40	48	88
Senqu River Valley	53	74	127	44	25	69
Total	280	448	728	131	123	254

reflectance analysis across sensors and time periods. Our choice of the Harmonized Sentinel-2 MSI, Level-1C (TOA) dataset was based on two primary considerations: (1) the widespread utility of Sentinel-2 MSI for water detection (Huang et al., 2018) and (2) the superior temporal coverage by TOA data compared to surface reflectance products for the Lesotho AEZs. The surface reflectance dataset due to its atmospheric correction exhibited significant data gaps, lacking imagery for 2017 and most of 2018, with frequent missing imagery in subsequent years.

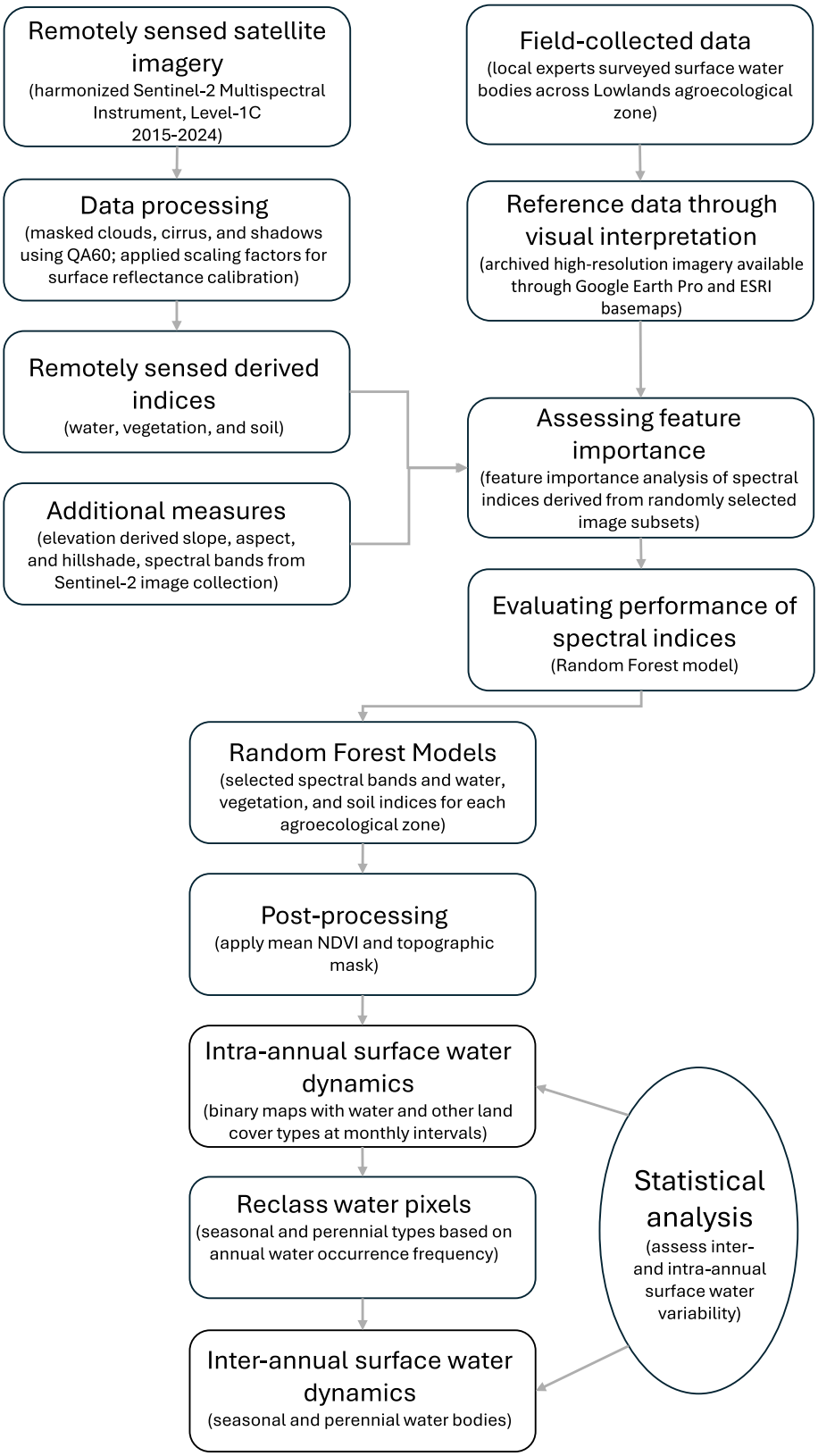

Fig. 2. Workflow for analyzing the spatiotemporal dynamics of seasonal and perennial surface water resources across Lesotho's diverse agroecological zones.

Moreover, cloud correction procedures applied to the surface reflectance products appeared to occasionally affect water pixels, diminishing classification accuracy relative to the TOA dataset.

We characterized surface waters at a monthly interval spanning from October 2015 to September 2024 (i.e., water year for Lesotho), by processing imagery in Google Earth Engine (GEE), with cloud interference minimized through the implementation of a cloud-masking algorithm employing the QA60 band, which provides cloud probability information at a 60-meter resolution. Pixels flagged as clouds or cirrus (i.e., bits 10 and 11) were excluded using a bitwise operation, and a binary mask was applied to isolate cloud-free pixels, which was then applied to the imagery. After filtering, the imagery was scaled to a reflectance range of 0 to 1, thereby normalizing the data for further quantitative analysis. Images with less than 20 % cloud cover across the study area were included to minimize data gaps. Monthly median composites were generated to mitigate the effects of residual cloud cover and shadows, ensuring consistent and reliable monitoring of water resources. We accessed the harmonized Sentinel-2 imagery archive using the *ee.ImageCollection* module, with *filterDate()* and *filterBounds()* applied for temporal and spatial filtering.

2.3.1. Remotely sensed derived water indices

To improve detection of water bodies from other land cover types for higher overall mapping accuracy, we evaluated a range of spectral indices targeting water, vegetation, and soil (Fig. 2; Table S2). Access to cloud computing resources like GEE enabled us to perform a systematic evaluation of multiple spectral indices, comparing their performance across various regions and time periods. The selection of these indices was driven by their ability to detect surface waters under varying environmental conditions while minimizing misclassification errors. We utilized NDWI and the green-SWIR variant of NDWI (referred to as MNDWI) in this study. Water-specific indices, such as NDWI, are widely applied for surface water extraction due to their reliance on NIR, SWIR, or green bands (Gao, 1996; McFEETERS, 1996; Xu, 2006). For example, Campos et al. (2012) demonstrated that NDWI derived from green band improved accuracy in mapping perennial water bodies, while the MNDWI, which replaces NIR with mid-infrared (MIR) bands, outperformed NDWI in detecting seasonal water bodies. This performance enhancement was attributed to the distinct spectral signatures of shallow water, aquatic vegetation, and sediments, which influence reflectance in the green and MIR portions of the electromagnetic spectrum, thus improving seasonal water detection (Soti et al., 2009).

However, NDWI is prone to misclassification, particularly in the presence of shadows or dark surfaces. To address this limitation, we incorporated the AWEI, which uses blue, green, SWIR, and NIR bands to enhance the distinction between water and non-water pixels, especially in areas with complex topography and urban environments (Feyisa et al., 2014). Moreover, given the snow-covered peaks in Mountains AEZ, we integrated the WRI, which combines red, green, NIR, and SWIR bands to improve water detection in areas where snow and shadow complicate water mapping (Shen and Li, 2010). Khalid et al. (2021) found that WRI outperformed both NDWI and AWEI in snow-covered regions, making it especially suitable for the Mountains AEZ of Lesotho. Further enhancing water detection, we used the floating algae index (FAI), which was initially developed for detecting algal blooms in open oceans but is also effective for identifying algal-rich shallow water bodies common near croplands (Hu, 2009). We also evaluated the normalized difference turbidity index (NDTI) for detecting shallow, highly turbid, or polluted water bodies, as standard water indices often fail to accurately highlight these (Bid and Siddique, 2019).

To mitigate misclassification between water and vegetation, we also employed vegetation indices like normalized difference vegetation index (NDVI) and enhanced vegetation index (EVI), especially in regions where dense aquatic vegetation exhibits spectral similarity to water surfaces. Additionally, the normalized difference moisture index (NDMI) was included to capture variations in vegetation surface water content. Bare soil indices, such as the bare soil index (BSI), were included to differentiate water from exposed land surfaces, while sand-related indices (the normalized differential sand dune index – NDSDI, normalized differential sand areas index – NDSAI, and normalized sand index – NSI), were considered to enhance the identification of riverbeds during the dry season, where exposed sediments could be confused with water (Secu et al., 2022).

To minimize misclassification in areas where topography complicates land cover detection and mapping (Huang et al., 2020), we applied terrain variables (e.g., aspect, slope, and hillshade) derived from NASA's 30 m SRTM digital elevation model (DEM) post-classification, rather than as input to the RF models. These topographic measures were derived using the *ee.Terrain.slope* and *ee.Terrain.hillshade* functions in GEE. For hillshade, we adjusted the illumination azimuth to 50° and altitude to 45° to better align with Lesotho's dominant solar geometry.

We excluded topographic variables from the RF models due to resolution and alignment concerns. Initial attempts to incorporate the 90 m SRTM DEM in GEE led to CRS transform mismatches with the Sentinel-2 imagery, causing edge artifacts and misalignments in the classification output. While adopting NASA's 30 m SRTM DEM resolved the alignment issue, its coarser resolution, compared to the 10–20 m spectral indices, introduced spatial artifacts. To prevent this, we applied topographic constraints only after classification (Hanshaw and Bookhagen, 2014; Li et al., 2022). This terrain-based post-classification mask removed pixels likely misclassified as water, specifically those on steep slopes or in persistent shadow. However, to preserve reservoirs—often located on steep terrain—we manually digitized reservoir polygons, expanding them slightly beyond their actual boundaries to account for potential variations in extent. These polygons were then subtracted from the terrain mask before application. Additionally, we refined mapping outcomes using a mean NDVI threshold. Pixels, initially classified as water, were reclassified as land (value = 0) if their mean NDVI exceeded 0.12, reflecting persistent vegetation cover unlikely to correspond to open water.

2.3.2. Constructing models for surface water mapping

We selected the RF algorithm (Breiman, 2001) for mapping surface waters due to its superior performance in handling complex, high-dimensional datasets with non-linear relationships, commonly encountered in remote sensing and hydrological applications. Its capacity to process both categorical and continuous data (Pal and Mather, 2005) makes it particularly suitable to experiment with a wide range of spectral indices and bands from remotely sensed satellite imagery, which, in this study, is essential for distinguishing water surfaces from other land cover types. Compared to other machine learning algorithms, such as support vector machines and decision trees, RF is particularly effective because it mitigates overfitting by aggregating multiple decision trees to improve generalization. Another key advantage is its insensitivity to data noise and missing values, which is particularly beneficial when working with satellite imagery affected by cloud cover or atmospheric distortions. RF functions by constructing an ensemble of decision trees, each trained on a random subset of the input data and a random subset of the predictor variables. This process of "bagging" and random feature selection ensures diversity among the trees, reducing correlation and enhancing generalization ability. This ensemble approach enhances predictive accuracy and reduces bias and variance, making it well-suited for distinguishing surface water from confounding land cover types like wetlands, bare soil, and vegetation (Belgiu and Drăguţ, 2016). Moreover, RF ranks the importance of input variables, enabling effective feature selection (Gislason et al., 2006). This capability is particularly advantageous for identifying the most suitable combination of spectral indices suitable for mapping surface waters across AEZs. Given these strengths, we selected RF for water surface mapping.

We developed robust RF models using 728 training points distributed across the four AEZs. To enhance model generalizability, we extracted spectral band and index values for each training point from multiple

randomly selected, harmonized Sentinel-2 images within our image collection. This approach substantially increased the temporal coverage and variability of our training points. This was done using the *sampleRegions()* function in GEE, which samples pixel values at the training point locations. Rather than relying on single scenes or composite images, this approach incorporated a diverse range of spectral variability and seasonal conditions, improving models' ability to generalize across different time periods. This approach addressed limitations in earlier methods, where models were trained separately on individual images or median composites, reducing the representativeness of the training data. The resulting dataset enabled the development of stable, zone-specific RF models with improved performance across varying temporal and environmental conditions.

Before developing RF models in GEE for each AEZ, we first conducted a variable importance analysis for each AEZ using the RF algorithm in Python to assess the comparative contribution of the selected spectral indices for the study. This analysis was performed on the tabular training dataset (values from 728 training points sampled across random images; Fig. S2) exported from GEE, rather than directly on imagery. This allowed us to identify the most informative bands and indices for each AEZ. Variable importance was determined using the Gini impurity criterion, which ranks input variables based on their impact on the classification. For this step, we split the dataset into 70 % for training and 30 % for testing to ensure the rankings were based on generalizable patterns avoiding overfitting. Using variable importance, we developed eight RF models for each AEZ (Table 2), resulting in a total of 32 models, each using different combinations of water, vegetation, and soil indices. Five models maintained a consistent set of vegetation and soil indices or bands while varying the water indices, with one model combining all water indices. The remaining three models were constructed using variable importance ranks (Fig. S3) to select combinations that minimized redundancy and avoided highly correlated variables (Fig. S4).

We mapped surface water using the RF algorithm at a monthly interval throughout the study period using the *ee.Classifier.smileRandomForest()* function in GEE. To optimize model performance, we initially trained the RF classifier with 100 trees and observed improved classification accuracy when increasing to 200 trees. However, further increasing to 300 trees did not yield any significant enhancement in accuracy, indicating diminishing returns. Therefore, we selected 200 trees for all final models to balance computational efficiency and classification accuracy.

2.4. Model performance and statistical analysis

2.4.1. Evaluating the performance of classification models

To assess model performance, we validated the mapped water cover using an independent testing dataset (n = 254) specific to each AEZ (Fig. 1; Table 1). For every mapped water cover, predicted class labels were sampled at the corresponding testing point locations. A confusion matrix was then generated using *ee.ConfusionMatrix()* to compare mapped and reference labels. From this matrix, overall accuracy—defined as the proportion of correctly classified samples—was computed and stored as image metadata.

This validation process was applied across all eight models developed for each AEZ, generating a monthly time series of overall accuracy for each model from the 2016 to 2024 water years. These accuracy values were exported as a CSV file for post-processing. To statistically evaluate the performance of different models, we applied a non-parametric Kruskal–Wallis test on the accuracy distributions, which informed the selection of the best-performing model for each AEZ (McKight and Najab, 2010).

Beyond quantitative accuracy assessment, we conducted a thorough visual inspection of the classification outputs. To support this evaluation, we utilized the HydroRIVERS shapefile (Lehner and Grill, 2013) for Lesotho to identify expected river and stream locations. This spatial reference allowed for a focused assessment of hydrologically relevant areas within the broader landscape, improving the evaluation of how well each model captured known surface water features.

Table 2
Sentinel imagery bands and derived water, vegetation, and soil indices used in constructing Random Forest models for each agroecological zone to determine the optimal index combination for accurately mapping surface water.

Random Forest model	Agroecological zone	Combination of Sentinel imagery spectral bands and derived water, vegetation, and soil indices used as remotely sensed variables
M1	Lowlands	B12, B8, B2, NDVI, BSI, NDWI
M2		B12, B8, B2, NDVI, BSI, MNDWI
M3		B12, B8, B2, NDVI, BSI, WRI
M4		B12, B8, B2, NDVI, BSI, AWEI
M5		B12, B8, B2, NDVI, BSI, NDWI, MNDWI, WRI, AWEI
M6		B12, B8, B2, NSI, BSI, MNDWI, WRI, AWEI, NDMI, FAI
M7		B12, B8, B2, NSI, BSI, NDSDI, WRI, AWEI, NDMI, FAI
M8		B12, B8, B2, NSI, BSI, MNDWI, WRI, AWEI, NDMI, FAI, NDVI
M1	Foothills	B12, B8, B3, NDVI, NDSAI, EVI, FAI, BSI, NDWI
M2		B12, B8, B3, NDVI, NDSAI, EVI, FAI, BSI, MNDWI
M3		B12, B8, B3, NDVI, NDSAI, EVI, FAI, BSI, WRI
M4		B12, B8, B2, NDVI, NDSAI, EVI, FAI, BSI, AWEI
M5		B12, B8, B2, NDVI, NDSAI, EVI, FAI, BSI, NDWI, MNDWI, WRI, AWEI
M6		B12, B8, B3, BSI, NDSAI, EVI, WRI, AWEI, NDMI, FAI
M7		B4, B8, B3, NDSAI, NDVI, WRI, AWEI, NDMI
M8		B11, B8, NDSDI, NDVI, EVI, NDWI, WRI
M1	Mountains	B11, B8, B3, NDSDI, NDVI, NDWI
M2		B11, B8, B3, BSI, NDVI, MNDWI
M3		B11, B8, B3, BSI, NDVI, WRI
M4		B11, B8, B3, NDSDI, NDVI, AWEI
M5		B11, B8, B3, NDVI, BSI, NDWI, MNDWI, WRI, AWEI
M6		B12, B8, B3, NSI, EVI, FAI, NDMI, AWEI, NDWI, NDSDI
M7		B11, B8, EVI, NDVI, WRI, NDWI, AWEI, MNDWI
M8		B11, B8, NDVI, EVI, AWEI, WRI, NDWI
M1	Senqu River Valley	B11, B8, B3, NDVI, NDSDI, NDWI
M2		B11, B8, B3, NDVI, NDSDI, MNDWI
M3		B11, B8, B3, NDVI, NDSDI, AWEI
M4		B11, B8, B3, NDVI, NDSDI, WRI
M5		B11, B8, B3, NDVI, NDSDI, NDWI, MNDWI, AWEI, WRI
M6		B11, B8, B12, AWEI, WRI, FAI, NDVI
M7		B8, B3, EVI, NDVI, NDSAI, EVI, AWEI, NDMI, FAI
M8		B11, B4, NDVI, MNDWI, WRI, AWEI

NDVI = normalized difference vegetation index; BSI = bare soil index; NDWI = normalized difference water index; MNDWI = modified normalized difference water index; WRI = water ratio index; AWEI = automated water extraction index; NSI = normalized sand index; NDMI = normalized difference moisture index; FAI = floating algae index; NDSDI = normalized differential sand dune index; NDSAI = normalized differential sand areas index; EVI = enhanced vegetation index.

2.4.2. Interannual variability of seasonal and perennial water bodies

We categorized mapped surface water into no water, seasonal surface water, and perennial surface water types. To ensure data reliability, we excluded mapped surface water with classification accuracy below 80 %, which was primarily affected by cloud cover, a factor known to impact classification accuracy. Additionally, pixels with fewer than four valid observations within a given year were excluded to reduce uncertainty in the classification process. Seasonal water was assigned to pixels where water occurred in fewer than 75 % of the monthly classifications. For perennial water, the occurrence had to exceed 75 %, with water

present at least once during each of the three defined periods: Wet (January–March), Moderate Dry (April–June), and Dry (July–September). These periods are defined by dividing the water year into quartiles based on temporal distribution. The first quartile (October–December; wet season) was excluded from this analysis due to frequent low-quality satellite imagery during this period. We hypothesized that both seasonal and perennial water bodies would consistently exhibit water presence during the wet season. If a pixel met the ≥ 75 % water occurrence threshold but lacked water presence in any one of the time periods, it was reclassified as seasonal surface water. This stringent approach effectively minimized the inclusion of transient water bodies and ensured that only water bodies that persisted across all periods were categorized as perennial.

To examine interannual variability in seasonal and perennial water bodies, we stacked monthly classified images for each water year of the study period (2016–2024 water years). To calculate the area of each water type, we used the *ee.Image.pixelArea()* function in GEE to generate per-pixel area values, which were then converted to square kilometers. These area values were added to the water maps using *addBands*, and the total area for each water type was computed with *reduceRegion* using a grouped sum reducer (*ee.Reducer.sum().group()*). This approach allowed us to aggregate the total areas of non-water, seasonal, and perennial water types within the study region for each annual thematic land cover. The resulting statistics were then exported for further analysis. In R, we summed seasonal and perennial water for each time step and applied the Mann-Kendall trend test and the Sen's Slope estimator to assess trends in surface water over time. These non-parametric methods were selected for their suitability in analyzing short time series (less than 10 years) and their robustness to non-normality and outliers, common in satellite-derived environmental datasets. The Mann-Kendall test identifies the statistical significance of monotonic trends (i.e., increasing or decreasing), while Sen's Slope estimator calculates the median rate of change per year. These methods are widely applied in hydrological and environmental studies with sparse, noisy, or nonlinear data (Mohammad et al., 2022; Phuong et al., 2020). Trend analyses were performed separately for perennial, seasonal, and total surface water within each AEZ to account for regional heterogeneity in water dynamics. All statistical analyses were conducted using R (R Core Team, 2024).

2.4.3. Intra-annual variability of surface water

To assess intra-annual variability in surface water, we applied several statistical tests to the monthly mapped surface water for each AEZ. We distinguish between two key aspects: variability, which refers to the fluctuation in surface water area across months within a year, and distribution, which describes the seasonal allocation of water throughout the year. Variability is indicated by the degree of fluctuation in water area from month to month. If the water area remains relatively constant throughout the year, it signifies low variability. Conversely, substantial fluctuations, with significant expansions during certain months and contractions in others, reflect high variability. To quantify variability, we used Levene's test, Bartlett's test, and Fligner-Killeen test to determine if the variance in monthly surface water area differed significantly between years. These tests were selected for their complementary strengths. For example, Bartlett's test is most effective under the assumption of normality (Aslam, 2020), Levene's test is more robust to deviations from normality (Schultz, 1985), and the Fligner-Killeen test is nonparametric offering greater robustness to non-normal or skewed distributions (Fligner and Killeen, 1976). Using all three tests provides a more comprehensive and reliable evaluation of changes in variability under varying data conditions.

Distribution, on the other hand, examines the seasonal pattern of water occurrence. For instance, a year where water peaks in summer and declines in winter may exhibit a different pattern compared to a year where the peak occurs in spring, even if overall water availability is similar. To evaluate changes in distribution, we used the Kruskal-Wallis test, a non-parametric method that assesses whether the seasonal pattern of water area across months has shifted significantly over time (McKight and Najab, 2010). A significant result from this test indicates a change in the temporal distribution of water within a year. We implemented all statistical analyses in R using zonal statistics results exported from GEE.

3. Results

3.1. Spectral indices contributing to the surface water mapping

The Kruskal–Wallis test found no significant differences among the RF models (Table 2) accuracy within any AEZ ($p > 0.05$; Table S3), indicating comparable performance (Fig. 3). This consistency likely reflects the careful selection of spectral indices and a large training dataset that improved generalizability. However, visual inspection revealed classification discrepancies, notably land misclassified as water (false positives), which can significantly overestimate water extent. Seasonal accuracy variations were significant for the Lowland ($p = 0.012$) and SRV ($p = 0.013$) AEZs, but post-hoc tests showed no significant month-to-month differences after Bonferroni correction, suggesting limited seasonal effects (Table S4).

The WRI was the most effective in RF models for mapping surface water across AEZs in distinguishing water bodies from rangeland, cropland, and bare soil (Fig. S3, 5). Seasonal variations and misclassifications had a minor impact on model performance. Additional indices—AWEI, NDWI, MNDWI, and vegetation indices—further improved water delineation. AWEI was excluded from the Foothills AEZ due to minimal urbanization and higher tree cover, where NDWI, WRI, NDVI, EVI, and NDSDI were more effective. In the Mountains AEZ, NDWI, WRI, NDVI, and EVI enhanced water detection in vegetated and shadowed areas. MNDWI was favored in the Lowlands and SRV AEZs, where NDWI struggled with built-up areas and bright exposed soils. Despite NDVI's lower importance in Lowlands RF models, it improved water-cropland differentiation. Most AEZ models retained Band 8 (NIR) and Band 11 (SWIR2) for their strong spectral contrast with water. While our approach aimed to minimize indices, the Lowlands AEZ RF model required additional indices—NDMI, NSI, and FAI—for improved classification accuracy and visual assessment due to its complex land cover (Table 3).

A total of 405 monthly mapped water surfaces were retained across all AEZs (Fig. 4) after excluding those with accuracy below 80 %. The mean overall accuracy was 92.5 % (SD = 0.0423), with a range of 80.4 % and 100 %. Among the AEZs, the SRV zone had the highest mean

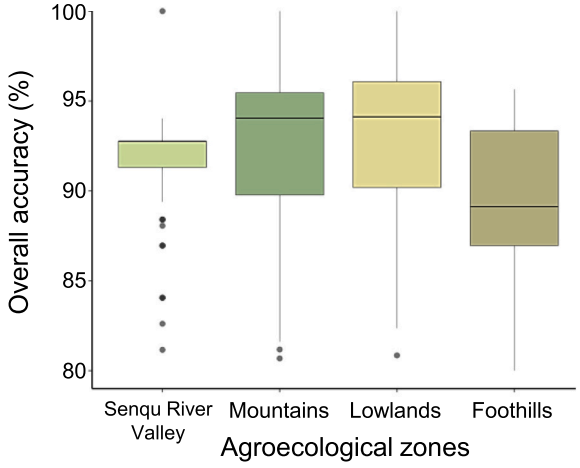

Fig. 3. Boxplots of overall accuracies from Random Forest models for each agroecological zone (AEZ) of Lesotho from the 2016 to 2024 water years, illustrating mapping performance across AEZs. Overall accuracies reflect mapped water cover exceeding 80%.

Table 3
The best-performing combinations of water, vegetation, and soil indices along with bands derived from the harmonized Sentinel-2 imagery for each agroecological zone of Lesotho.

Agroecological zones (AEZs)	Best performing combination of bands and indices
Lowlands	B12, B8, B2, MNDWI, WRI, AWEI, NDMI, NSI, FAI, BSI, NDVI
Foothills	B11, B8, NDWI, WRI, NDSDI, NDVI, EVI
Mountains	B8, B11, WRI, AWEI, NDWI, NDVI, EVI
Senqu River Valley	B11, B4, MNDWI, WRI, AWEI, NDVI

MNDWI = modified normalized difference water index; WRI=water ratio index; AWEI=automated water extraction index; NDMI=normalized difference moisture index; NSI = normalized sand index; FAI = floating algae index; BSI=bare soil index; NDVI=normalized difference vegetation index; NDWI = normalized difference water index; NDSDI = normalized differential sand dune index. EVI=enhanced vegetation index.

accuracy (94.4 %) and the lowest variability (SD = 0.0258), with a median accuracy of ~ 96 %. In contrast, the Foothills zone had the lowest mean accuracy (89.5 %) and moderate variability (SD = 0.0382), with accuracy ranging from 80.4 % and 95.7 %. The Lowlands and Mountains zones had comparable mean accuracies of ~ 93 %, though the Lowlands zone exhibited the highest variability (SD = 0.0457), indicating greater fluctuation in accuracy (Fig. 3, Table S5).

3.2. Interannual trends in surface water dynamics across AEZs

Analysis of mapping outcomes from the water year 2016 to 2024 revealed a general increase in total surface water area across all AEZs. However, analysis indicated that this increasing trend achieved statistical significance ($p < 0.05$) only in the SRV region (Fig. 5; Table S6). Disaggregating the data into seasonal and perennial water bodies, however, uncovered distinct temporal patterns across AEZs. In the Foothills AEZ, perennial water bodies exhibited a statistically significant increasing trend with a Sen's slope of 0.314 km^2/year ($p = 0.0187$). This finding indicates a robust expansion of permanent water features in this region. In contrast, seasonal water bodies showed no statistically significant change over the study period, suggesting stability in ephemeral water features despite climate variability. The Lowlands AEZ displayed no statistically significant trends for either perennial or seasonal water bodies. The Mountains AEZ revealed contrasting dynamics between seasonal and perennial water bodies. Perennial water bodies demonstrated a significant increase with a Sen's slope = 6.03 km2/year ($p = 0.0354$), representing the largest rate of expansion among all AEZs. Conversely, seasonal water bodies exhibited a marginally significant declining trend with a Sen's slope of −1.15 km^2/year ($p = 0.0635$). This inverse relationship suggests a potential conversion of seasonal water bodies to perennial status or different drivers affecting each water type. The SVR AEZ was the only region to show a statistically significant upward trend in total water area ($p = 0.028$), with a Sen's slope of 0.58 km^2/year; however, when disaggregated, both perennial and seasonal water types showed non-significant trends moving in opposite directions (Table S6). This finding suggests complex and potentially counterbalancing hydrological processes operating within this zone. Overall, these findings highlight the heterogeneity of surface water trends across AEZs and surface water types, with perennial water bodies constantly contributing to overall increases, while seasonal water exhibited greater variability and occasional declines, suggesting the need for localized water resource assessments to account for dynamic and region-specific hydrological changes.

3.3. Intra-annual trends in surface water dynamics

Surface water dynamics exhibit distinct regional patterns, with some zones experiencing changes in both variability and seasonal distribution, while others show shifts primarily in distribution (Fig. 6, 7). These findings emphasize the need for region-specific water management

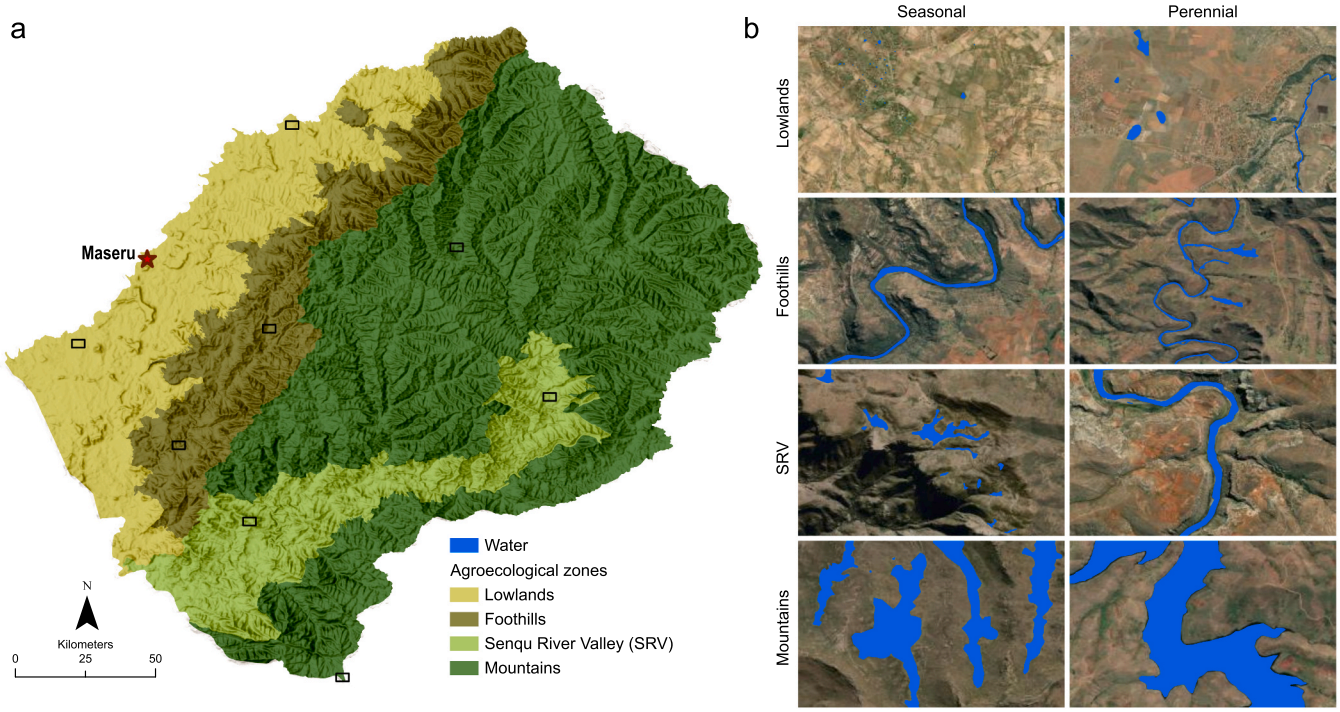

Fig. 4. Surface water from Random Forest models using the best index combination for each agroecological zone (AEZ). (a) A reference map of Lesotho shows sample locations, with AEZ boundaries in gray and sampled regions in black. (b) The left column shows seasonal mapped water, while the right column displays perennial water bodies. All images are from October 2024. Due to the large size of the AEZs, only representative portions are shown, though classification was conducted nationwide.

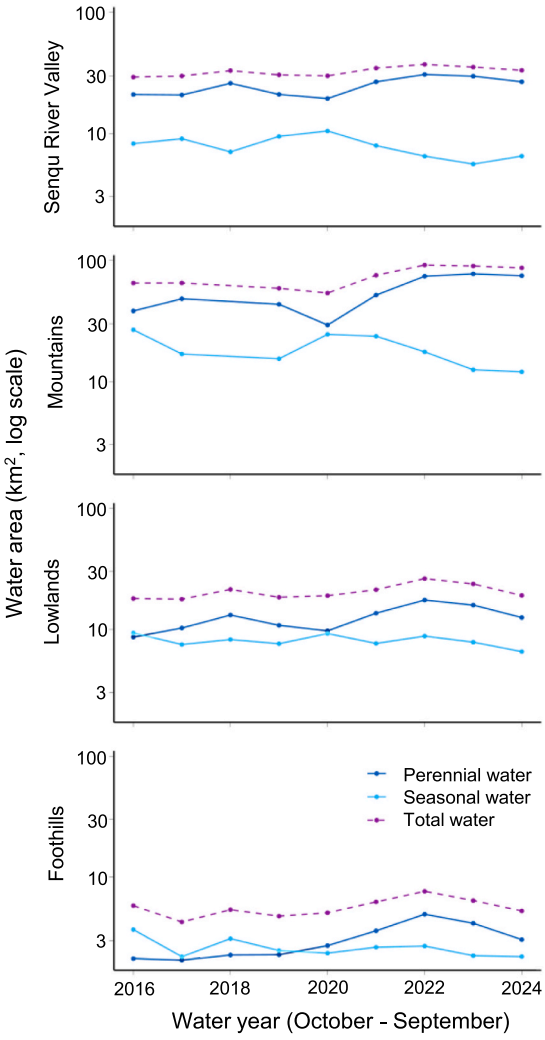

Fig. 5. Trends in seasonal, perennial, and total surface water across Lesotho's agroecological zones (AEZs) from the 2016 to 2024 water years. Perennial water (navy line) represents areas where water was detected in over 75% of valid monthly observations and appeared in at least three out of four seasons (excluding October–December due to data gaps). Seasonal water (blue line) includes areas with 25% to 75% water occurrence or those exceeding 75% but present in fewer than three seasons. The total water area (purple dashed line) is the annual sum of perennial and seasonal surface water areas. Pixels with fewer than four valid monthly observations per year were excluded from the analysis. (For interpretation of the references to colour in this figure legend, the reader is referred to the web version of this article.)

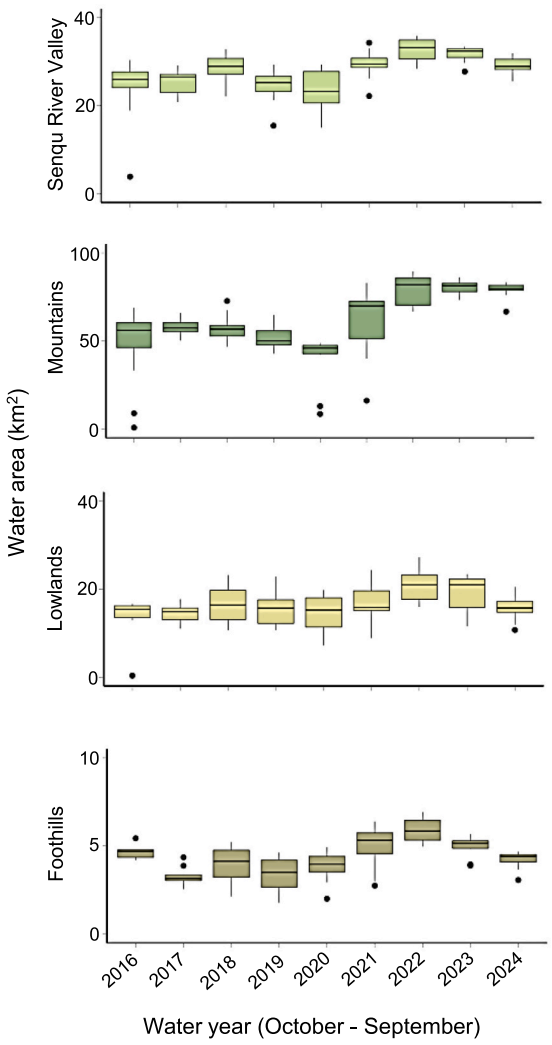

Fig. 6. Intra-annual variability in surface water area (km^2) across Lesotho's agroecological zones (AEZs) for each water year (October–September). Each AEZ shows variability in water area over time. Boxes indicate the interquartile range (IQR) with the median as a horizontal line, whiskers extend to 1.5 times the IQR, and points beyond represent outliers.

strategies to address evolving hydrological regimes. In the Foothills AEZ, all three variability tests yielded statistically significant results (Levene's $p = 0.040$; Bartlett's $p = 0.020$; and Fligner's $p = 0.049$), providing strong evidence of altered patterns in the spread of monthly surface water area between years (Fig. 6; Table S7). The consistency across these tests, which vary in their sensitivity to normality assumptions, reinforces the robustness of this finding. The Kruskal-Wallis test likewise returned a highly significant result ($p < 0.0001$), suggesting that substantial shifts have occurred in the seasonal distribution of surface water area over time (Table S7). This dual change in both variability and distribution suggests fundamental alterations in the hydrological regime of the Lowlands zone. The Lowlands AEZ displayed stable variability (all $p > 0.05$), but the Kruskal-Wallis test ($p = 0.001$) signaled a redistribution of water across months (Fig. 7), underscoring the importance of examining both aspects of hydrological change, as distribution patterns may evolve independently of variability characteristics.

In the Mountains AEZ, two variability tests were significant (Levene's $p = 0.045$, Bartlett's $p < 0.0001$) with Fligner-Killeen showing marginal significance ($p = 0.069$), indicating that monthly water area fluctuations have changed significantly between years. The strong significance in Bartlett's test particularly suggests pronounced changes in variance, though the more conservative Fligner-Killeen result indicates some uncertainty regarding the nature of these changes. The Kruskal-Wallis test was highly significant ($p < 0.0001$), confirming substantial shifts in seasonal distribution patterns of surface water. Together, these results point to comprehensive changes in both the magnitude and timing of water availability in the Mountains. The SRV AEZ showed mixed evidence for variability shifts, with Bartlett's test ($p < 0.0001$) detecting significant changes, while Levene's and Fligner's tests did not. However, despite the ambiguity in variability assessment, the Kruskal-Wallis test was highly significant ($p < 0.0001$), clearly demonstrating that distribution patterns of surface water have shifted considerably over time (Fig. 7). Together, the Foothills and Mountains exhibit strong evidence of changes in both variability and seasonal distribution, whereas the Lowlands and SRV regions primarily show distributional shifts. These trends underscore the need for spatially tailored water resource management strategies to address region-specific hydrological responses to environmental change (Fig. 6, Table S4).

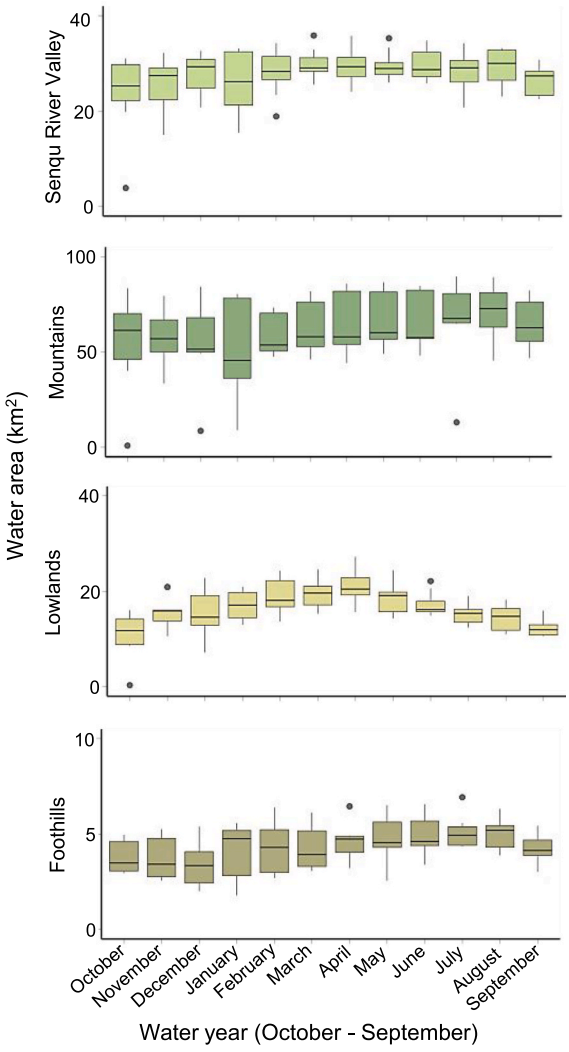

Fig. 7. Intra-annual distribution of surface water area (km^2) at monthly intervals across Lesotho's AEZs from 2016 to 2024 water year. Each AEZ shows intra-annual variations in water area throughout the year. Boxes represent the interquartile range (IQR), with the median as the horizontal line, whiskers extend to 1.5 times the IQR, and points beyond present outliers.

4. Discussion

Lesotho's abundant water resources hold substantial potential for agricultural development and climate adaptation, especially given that over 70 % of the population depends on agriculture for their livelihood. However, only 9 % of the country's total land is suitable for agriculture, and just 1.2 % of arable land is irrigated (Verschuur et al., 2021). As a result, farming remains largely rainfed, limiting productivity and increasing vulnerability to climate variability. This challenge is exacerbated by the sector's shift from subsistence grain farming to high-value horticultural crops, which have higher water demands. Despite past efforts, such as the Integrated Rural Development Projects of the 1970s, many donor-supported irrigation initiatives have collapsed after project completion due to limited funding and the high costs of maintaining systems like sprinklers, which are often unsustainable for smallholders (Rantšo, 2016; FAO, 2005; Moeti, 2007). Small-scale irrigation schemes often rely on seasonal rivers that dry up during droughts, leading to failure and reversion to rainfed farming. Even Lesotho's perennial water sources have proven unreliable during severe droughts, leading to increased food insecurity (Stevens & Ntai, 2011). Moreover, farmers receive minimal support from agricultural extension services, further limiting the success of irrigation initiatives. More recently, the Smallholder Development Project (phases 1 and 2, 2012–2018), jointly implemented by the World Bank and the Government of Lesotho, sought to address these issues by promoting irrigated horticulture through greenhouse farming. Given these persistent challenges, understanding the spatial and temporal dynamics of surface water is essential for improving water resource management and ensuring sustainable agricultural development. This study employs spectral indices from Sentinel imagery within an RF framework to accurately map and assess surface water dynamics in Lesotho, providing essential insights for sustainable water management in a changing climate. By distinguishing between seasonal and perennial water bodies, we have provided valuable insights into the spatiotemporal variability of water resources across diverse AEZs. The primary finding of this research is the heterogeneous nature of water dynamics across AEZs, which emphasizes the importance of region-specific water resource assessments to address the challenges posed by climate variability and hydrological changes.

Effective surface water mapping relies on selecting appropriate spectral indices to capture spatiotemporal variability and support resource management. This study identified the most effective index combinations for each AEZ in Lesotho, achieving on average 92 % accuracy across RF models. The WRI consistently performed best across AEZs, particularly when combined with AWEI, NDWI, MNDWI, and vegetation-based indices, enhancing the distinction between water and mixed land cover. These findings align with prior research (Tesfaye and Breuer, 2024; Wen et al., 2021), which emphasizes the benefits of multi-index approaches due to complex interactions between water, vegetation, and soil reflectance. These results align with Al-Ali et al. (2024), who found that combining indices improves accuracy because no single index captures all water-related changes, especially in mixed or shadowed areas. AWEI frequently outperformed NDWI and MNDWI in surface water extraction (Feyisa et al., 2014; Laonamsai et al., 2023; Tesfaye and Breuer, 2024), especially in shadow-prone, mountainous regions (Laonamsai et al., 2023), while Xie et al. (2016) found that combining the morphological shadow index with NDWI improved accuracy. However, NDWI sometimes surpassed AWEI and WRI in specific contexts (Khalid et al., 2021; Serrano et al., 2019), reinforcing the need for context-specific index selection. In the Lowlands AEZ, NDMI, NSI, and FAI improved accuracy, though seasonal variability affected performance, consistent with findings by Mohammadi et al. (2017). NDVI masking also enhanced classification, especially for shallow or seasonal water bodies, by reducing confusion with bare soil and fallow fields. Applying a mean NDVI threshold helped retain water pixels while minimizing misclassification. These results highlight the value of tailoring spectral index combinations and pre-processing steps by zone to improve classification accuracy. A multi-index strategy is especially important in diverse landscapes like Lesotho, where no single index can reliably capture all aspects of water body dynamics.

This study introduces a novel method for classifying surface water into seasonal and perennial categories that may contribute to the potential improvements to water allocation strategies during critical agricultural periods in water-scarce regions. Previous research indicates that seasonal water bodies are more sensitive to temperature fluctuations, while both seasonal and perennial water bodies are responsive to precipitation, underscoring the importance of spatiotemporal analysis for effective water management (Ayers et al., 2024; Wang et al., 2023). This aligns with Nyberg et al., (2024), who emphasize the necessity of accurately quantifying these dynamics for assessing ecosystem health and understanding the impacts of climate change and anthropogenic influences. In contrast to traditional classification methods, which rely on occurrence thresholds (e.g., $\geq$75 % for perennial), our approach offers an alternative. These thresholds, however, vary across studies (Cai et al., 2024; Wang et al., 2022; Zou et al., 2018) and are sensitive to the quality of satellite data, with cloud contamination introducing inconsistencies. Common gap-filling methods, such as kernel interpolation, may misclassify narrow river systems (Mullen et al., 2021), while

automatic backscatter thresholding using SAR data requires region-specific adjustments, presenting challenges in heterogeneous landscapes like Lesotho. To address these limitations, we employed a classification approach that does not rely on gap-filling. By maintaining a > 75 % threshold for perennial water bodies and introducing a requirement for at least one water observation per season, we reduced errors in narrow rivers, and enhanced classification accuracy.

Our spatiotemporal analysis revealed notable trends across AEZs. In the Lowlands, the growth of perennial water bodies suggests increased water permanence, likely due to rainfall shifts or interventions like rainwater harvesting (Ayers et al., 2024; Ketchum et al., 2023). In the Mountains AEZ, a decline in seasonal and rise in perennial water bodies point to hydrological changes or seasonal-to-perennial transitions (Zaremehrjardy et al., 2022). These patterns underscore the influence of both climate and human activity on water dynamics, emphasizing the need for integrated resource management (Ketchum et al., 2023). Between 2016 and 2024, surface water increased across all AEZs, with statistically significant gains in the SRV AEZ, driven mainly by perennial water bodies. Seasonal water showed more variability, with occasional declines. This highlights the importance of planning for both permanent water expansion and ephemeral water variability. Changes in river permanence also affect groundwater recharge and stability (Zaremehrjardy et al., 2022). However, the study has limitations. It may not fully capture the effects of extreme events, seasonal variability, or complex climate-human-hydrology interactions. Additionally, the spatial and temporal resolution may miss small or rapidly changing water bodies, pointing to the need for improved monitoring tools.

Statistical analysis of surface water dynamics reveals pronounced interannual and intra-annual variability across Lesotho's AEZs, reflecting complex hydrological shifts potentially driven by both climatic and anthropogenic factors. The Foothills AEZ exhibits significant changes in surface water distribution and variability, indicative of a fundamental reconfiguration of its hydrological regime, likely influenced by climate variability (Bao et al., 2019). In contrast, the Mountains AEZ demonstrates substantial variance fluctuations, signaling altered timing and magnitude of water availability. These spatially heterogeneous trends underscore the urgency of implementing region-specific water resource management strategies. Monthly surface water trends across AEZs confirm strong seasonal patterns, aligning with Xu (2006), who establishes a direct linkage between hydrological variability and climate conditions. The observed increase in surface water extent in the Lowlands AEZ suggests either enhanced water retention through anthropogenic interventions or shifts in precipitation and runoff patterns (DeFries and Eshleman, 2004). However, distinguishing between climatic influences and human-driven modifications, such as reservoir operations and irrigation expansion, remains methodologically challenging, reinforcing the need for high-resolution remote sensing and ground-based validation.

The disproportionate greater increase in perennial water bodies compared to seasonal ones across all AEZs indicates that infrastructure-driven hydrological changes (i.e., human-made dams and reservoirs) have had a stronger impact than climate-induced variability. If climate were the primary driver, we would expect similar trends in both seasonal and perennial water bodies. This interpretation is supported by earlier development initiatives—particularly in the Lowlands—where many small reservoirs were created through community development and food-for-work projects starting in the 1980 s. These efforts are aimed at harvesting stormwater for livestock and small-scale irrigation. This pattern aligns with recent studies, such as Palazzoli et al., (2023), which highlight the dominant role of human interventions in shaping surface water extent, and Nyberg et al., (2024), who found that seasonal water variation is more closely linked to human interventions than to climate shifts. Despite the presence of major projects like the Lesotho Highlands Water Project, nearby communities receive limited benefits, as much of the water is primarily exported rather than used locally for irrigation or domestic needs. As a result, subsistence farming remains highly vulnerable—dependent on unpredictable rainfall, frequently disrupted by droughts, and further constrained by delayed rains that affect planting and crop development. These challenges underscore the importance of maintaining stable natural surface water flows (streamflow) and improving local water access to enhance agricultural resilience.

These findings highlight the need for future research to quantify the relative roles of human and climatic drivers, informing evidence-based water governance and adaptive management. A key limitation in surface water mapping is the underestimation of ephemeral water bodies, often due to persistent cloud cover or complex terrain (Cao et al., 2024; Verdin, 1996). Ephemeral water bodies, due to their short duration, are more susceptible to omission, which can lead to an overrepresentation of perennial water bodies in analyses. To address this, the incorporation of higher-temporal-resolution satellite imagery, in conjunction with *in-situ* hydrological observations, is essential for improving classification accuracy and reducing observational biases (Cao et al., 2024). Integrating physical models and deep learning also offers promise (Sigopi et al., 2024; Sun et al., 2024). Rising surface water in the Foothills, Mountains, and SRV calls for further statistical interrogation to determine its persistence and implications for long-term hydrological stability. While these trends may reflect improvements in water retention or localized climatic shifts, distinguishing transient fluctuations from systemic hydrological transformations is essential. Conversely, the Lowlands show stable trends and variability, but significant shifts in seasonal distribution highlights underlying changes that merit further investigation. Examining traditional and contemporary water management practices in these regions could provide scalable insights for enhancing water security in more vulnerable landscapes.

The Mann-Kendall test indicates a possible but statistically insignificant increase in surface water at the national level ($p = 0.20$), highlighting the need for deeper analysis of water dynamics in Lesotho. As Green et al. (2011) emphasized, continuous monitoring is crucial to assess climate change impacts on water resources. Understanding how shifts in rainfall patterns and land use affect water availability is essential for developing adaptive water management strategies. The Kruskal-Wallis test shows significant seasonal variation in surface water coverage, particularly in the Foothills, Mountains, and SRV. These findings are consistent with Twisa and Buchroithner (2019), who observed substantial seasonal fluctuations in water availability. Such variability may stem from changing precipitation, evaporation rates, and reservoir operations, all of which influence irrigation planning and agricultural productivity. Identifying periods of peak water availability, for example, could help improve irrigation efficiency. All AEZs showed seasonal shifts, but intra-annual variability varied regionally, indicating uneven surface water dynamics. This stability may result from consistent rainfall patterns or lower evaporation linked to cooler temperatures at higher elevations. Investigating these stable regimes could offer transferable lessons in land and water management, especially for improving resilience in more vulnerable or variable environments affected by climate change.

Despite the successes of this approach, challenges persist. Classification discrepancies, such as false positives where land was misclassified as water, highlight the need for further refinement of spectral indices and machine learning models. Limitations in model performance are partly attributed to its inability to effectively capture small, seasonal water bodies, especially in regions with complex topographies (Ogilvie et al., 2018). These transient water bodies are difficult to detect due to their size and variability throughout the year (Sawaya et al., 2003). In areas like the Mountains of Lesotho, steep elevation gradients and rugged terrain can confound spectral signatures due to surrounding vegetation, shadows, and mixed land cover (Feyisa et al., 2014). Visual assessments of the model's output confirm that some small water bodies were not consistently identified. Additionally, seasonal accuracy variations suggest the model's sensitivity to subtle surface water changes is limited in areas with complex land cover. This indicates that while the

model performs well overall, further refinement is needed to improve detection accuracy in these challenging contexts. Incorporating higher-resolution data or contextual layers such as soil moisture and vegetation dynamics could enhance the model's ability to capture smaller hydrological features. Despite these limitations, the overall consistency of the random forest model across AEZs indicates its generalizability to regions with similar environmental conditions. The findings hold significant policy implications for Lesotho and similar regions in Sub-Saharan Africa. Remote sensing-based monitoring of surface water can inform data-driven policies supporting water storage infrastructure, climate-smart agriculture, and community-based water governance. Understanding the spatiotemporal dynamics of surface water is vital for addressing water scarcity, particularly in areas where climate change exacerbates existing stressors. Identifying regional water availability trends can guide the development of tailored, sustainable water resource management strategies.

5. Conclusions

This study provides a comprehensive assessment of surface water dynamics in Lesotho, employing spectral indices and machine learning techniques to map seasonal and perennial water resources across diverse AEZs. By leveraging Sentinel imagery and RF models, we successfully identified key spectral indices, such as the WRI, NDWI, and MNDWI, that effectively delineate water bodies in diverse AEZs. The ability to distinguish between seasonal and perennial surface waters represents a significant advancement in monitoring spatiotemporal water fluctuations. Our findings highlight the increasing trend of surface water in certain regions, particularly in the SRV and Mountains AEZs, where perennial water bodies are expanding. This provides valuable insight into long-term hydrological changes that can inform water resource management strategies.

The results underscore the importance of localized water resource assessments, as surface water dynamics vary considerably across regions. In particular, the Lowlands AEZ showed significant changes in both the variability and distribution of water bodies, suggesting alterations in the hydrological regime, whereas other AEZs like the Foothills and SRV revealed more nuanced shifts in distribution patterns. These findings emphasize the need for region-specific water management policies that account for these spatiotemporal changes, particularly in areas facing growing water scarcity due to climate change and population pressures.

Our study offers important implications for water governance in Sub-Saharan Africa. The capacity to monitor surface water with remote sensing techniques can support the development of data-driven policies that promote sustainable water management. Future work should focus on expanding this analysis to other regions with similar climatic conditions, further improving the classification accuracy through multi-source data fusion. Additionally, investigating the drivers behind the observed shifts in seasonal and perennial water bodies, including land-use changes and climate variability, could provide deeper insights into the evolving hydrological processes that affect water availability and its management in the face of climate change. Finally, further integration of remote sensing data with hydrological modeling could improve predictions of future water dynamics, thus enhancing regional cooperation and supporting effective climate-smart water policies.

CRediT authorship contribution statement

Kunwar K. Singh: Writing – review & editing, Writing – original draft, Visualization, Supervision, Software, Resources, Methodology, Funding acquisition, Formal analysis, Conceptualization. **Sayedeh Sara Sayedi:** Writing – review & editing, Methodology, Formal analysis. **Ariel BenYishay:** Writing – review & editing, Funding acquisition, Conceptualization, Supervision, Software, Resources. **Tšepiso A. Rantšo:** Writing – review & editing, Resources.

Declaration of competing interest

The authors declare that they have no known competing financial interests or personal relationships that could have appeared to influence the work reported in this paper.

Acknowledgments

We would like to express our deepest gratitude to the Millennium Challenge Corporation for their financial support (Grant No.: 95332418 N00002), which made this research possible. We are especially grateful to Dr. Carly Muir for her tireless dedication and invaluable contributions throughout the project, ensuring its success at every stage. We extend our heartfelt thanks to the Research and Evaluation team for their consistent feedback and insightful recommendations, which greatly enriched the quality and impact of this work.

Appendix A. Supplementary material

Supplementary data to this article can be found online at https://doi.org/10.1016/j.jag.2025.104688.

Data availability

Data will be made available on request.

References

Acharya, T.D., Subedi, A., Huang, H., Lee, D.H., 2019. Application of Water Indices in Surface Water Change Detection using Landsat Imagery in Nepal. Sens. Mater. 31, 1429. https://doi.org/10.18494/SAM.2019.2264.

Al-Ali, Z., Abulibdeh, A., Al-Awadhi, T., Mohan, M., Al Nasiri, N., Al-Barwani, M., Al Nabbi, S., Abdullah, M., 2024. Examining the potential and effectiveness of water indices using multispectral sentinel-2 data to detect soil moisture as an indicator of mudflow occurrence in arid regions. Int. J. Appl. Earth Obs. Geoinf. 130, 103887. https://doi.org/10.1016/j.jag.2024.103887.

Amitrano, D., Di Martino, G., Di Simone, A., Imperatore, P., 2024. Flood detection with SAR: a review of techniques and datasets. Remote Sens. (Basel) 16, 656. https://doi.org/10.3390/rs16040656.

Aslam, M., 2020. Design of the Bartlett and Hartley tests for homogeneity of variances under indeterminacy environment. Journal of Taibah University for Science 14, 6–10. https://doi.org/10.1080/16583655.2019.1700675.

Ayers, J.R., Yarnell, S.M., Baruch, E., Lusardi, R.A., Grantham, T.E., 2024. Perennial and Non-Perennial Streamflow Regime Shifts across California, USA. Water Resour. Res. 60, e2023WR035768. https://doi.org/10.1029/2023WR035768.

Bangira, T., Alfieri, S.M., Menenti, M., Van Niekerk, A., 2019. Comparing thresholding with machine learning classifiers for mapping complex water. Remote Sensing 11 (11), 1351. https://doi.org/10.3390/rs11111351.

Bao, Z., Zhang, J., Wang, G., Chen, Q., Guan, T., Yan, X., Liu, C., Liu, J., Wang, J., 2019. The impact of climate variability and land use/cover change on the water balance in the Middle Yellow River Basin. China. Journal of Hydrology 577, 123942. https://doi.org/10.1016/j.jhydrol.2019.123942.

Belgiu, M., Drăguţ, L., 2016. Random forest in remote sensing: a review of applications and future directions. ISPRS J. Photogramm. Remote Sens. 114, 24–31. https://doi.org/10.1016/j.isprsjprs.2016.01.011.

Bentivoglio, R., Isufi, E., Jonkman, S.N., Taormina, R., 2022. Deep learning methods for flood mapping: a review of existing applications and future research directions. Hydrol. Earth Syst. Sci. 26, 4345–4378. https://doi.org/10.5194/hess-26-4345-2022.

Bhagat, V.S., Sonawane, K.R., 2011. Use of Landsat ETM+ data for delineation of water bodies in hilly zones. J. Hydroinf. 13, 661–671. https://doi.org/10.2166/hydro.2010.018.

Biazin, B., Sterk, G., Temesgen, M., Abdulkedir, A., Stroosnijder, L., 2012. Rainwater harvesting and management in rainfed agricultural systems in sub-Saharan Africa – a review. Physics and Chemistry of the Earth, Parts a/b/c 47–48, 139–151. https://doi.org/10.1016/j.pce.2011.08.015.

Bid, S., Siddique, G., 2019. Identification of seasonal variation of water turbidity using NDTI method in Panchet Hill Dam, India. Modeling Earth Systems and Environment 5, 1179–1200. https://doi.org/10.1007/s40808-019-00609-8.

Breiman, L., 2001. Random forests. Machine Learning 45, 5–32. https://doi.org/10.1023/A:1010933404324.

Cai, Y., Shi, Q., Liu, X., 2024. Spatiotemporal Mapping of Surface Water using Landsat Images and Spectral Mixture Analysis on Google Earth Engine. J Remote Sens 4, 0117. https://doi.org/10.34133/remotesensing.0117.

Campos, J.C., Sillero, N., Brito, J.C., 2012. Normalized difference water indexes have dissimilar performances in detecting seasonal and permanent water in the

Sahara–Sahel transition zone. J. Hydrol. 464–465, 438–446. https://doi.org/10.1016/j.jhydrol.2012.07.042.
Cao, H., Tian, Y., Liu, Y., Wang, R., 2024. Water body extraction from high spatial resolution remote sensing images based on enhanced U-Net and multi-scale information fusion. Sci. Rep. 14, 16132. https://doi.org/10.1038/s41598-024-67113-7.
Chen, K., Chen, H., Zhou, C., Huang, Y., Qi, X., Shen, R., Liu, F., Zuo, M., Zou, X., Wang, J., Zhang, Y., Chen, D., Chen, X., Deng, Y., Ren, H., 2020. Comparative analysis of surface water quality prediction performance and identification of key water parameters using different machine learning models based on big data. Water Res. 171, 115454. https://doi.org/10.1016/j.watres.2019.115454.
DeFries, R., Eshleman, K.N., 2004. Land-use change and hydrologic processes: a major focus for the future. Hydrol. Process. 18, 2183–2186. https://doi.org/10.1002/hyp.5584.
De Pauw, E., Göbel, W., Adam, H., 2000. Agrometeorological aspects of agriculture and forestry in the arid zones. Agric. For. Meteorol. 103, 43–58. https://doi.org/10.1016/S0168-1923(00)00118-0.
FAO., 2005. AQUASTAT Country Profile – Lesotho. Rome: Italy. https://openknowledge.fao.org/server/api/core/bitstreams/fa42c013-a037-47df-8ac3-d7170b4346b7/content.
Feyisa, G.L., Meilby, H., Fensholt, R., Proud, S.R., 2014. Automated Water Extraction Index: a new technique for surface water mapping using Landsat imagery. Remote Sens. Environ. 140, 23–35. https://doi.org/10.1016/j.rse.2013.08.029.
Fligner, M.A., Killeen, T.J., 1976. Distribution-free two-sample tests for scale. J. Am. Stat. Assoc. 71, 210–213.
Gao, B., 1996. NDWI—A normalized difference water index for remote sensing of vegetation liquid water from space. Remote Sens. Environ. 58, 257–266. https://doi.org/10.1016/S0034-4257(96)00067-3.
Gislason, P.O., Benediktsson, J.A., Sveinsson, J.R., 2006. Random Forests for land cover classification. Pattern Recogn. Lett. 27, 294–300. https://doi.org/10.1016/j.patrec.2005.08.011.
Grafton, R.Q., Williams, J., Perry, C.J., Molle, F., Ringler, C., Steduto, P., Udall, B., Wheeler, S.A., Wang, Y., Garrick, D., Allen, R.G., 2018. The paradox of irrigation efficiency. Science 361, 748–750. https://doi.org/10.1126/science.aat9314.
Green, T.R., Taniguchi, M., Kooi, H., Gurdak, J.J., Allen, D.M., Hiscock, K.M., Treidel, H., Aureli, A., 2011. Beneath the surface of global change: Impacts of climate change on groundwater. J. Hydrol. 405, 532–560. https://doi.org/10.1016/j.jhydrol.2011.05.002.
Guo, Q., Pu, R., Li, J., Cheng, J., 2017. A weighted normalized difference water index for water extraction using Landsat imagery. Int. J. Remote Sens. 38, 5430–5445. https://doi.org/10.1080/01431161.2017.1341667.
Gwimbi, P., Rakuoane, T.E., 2019. Impacts of Dams on Downstream Riparian Ecosystems' Health and Community Livelihoods: a Case of the Lesotho Highlands Water Project. In: Bamutaze, Y., Kyamanywa, S., Singh, B.R., Nabanoga, G., Lal, R. (Eds.), Agriculture and Ecosystem Resilience in Sub Saharan Africa, Climate Change Management. Springer International Publishing, Cham, pp. 257–276. https://doi.org/10.1007/978-3-030-12974-3_12.
Haas, E.M., Bartholomé, E., Combal, B., 2009. Time series analysis of optical remote sensing data for the mapping of temporary surface water bodies in sub-Saharan western Africa. J. Hydrol. 370, 52–63. https://doi.org/10.1016/j.jhydrol.2009.02.052.
Hanshaw, M.N., Bookhagen, B., 2014. Glacial areas, lake areas, and snow lines from 1975 to 2012: status of the Cordillera Vilcanota, including the Quelccaya Ice Cap, northern central Andes, Peru. Cryosphere 8, 359–376. https://doi.org/10.5194/tc-8-359-2014.
Herndon, K., Muench, R., Cherrington, E., Griffin, R., 2020. An Assessment of Surface Water Detection Methods for Water Resource Management in the Nigerien Sahel. Sensors 20, 431. https://doi.org/10.3390/s20020431.
Hlalele, B.M., 2017. Cointegration analysis of vulnerability index and standardised precipitation index in Mafeteng district. Lesotho. Jàmbá 9. https://doi.org/10.4102/jamba.v9i1.330.
Hoag, C., 2019. "Water is a gift that destroys": making a national natural resource in Lesotho. Economic Anthropology 6, 183–194. https://doi.org/10.1002/sea2.12149.
Hu, C., 2009. A novel ocean color index to detect floating algae in the global oceans. Remote Sensing of Environment 113 (10), 2118–2129. https://doi.org/10.1016/j.rse.2009.05.012.
Huang, C., Chen, Y., Zhang, S., Wu, J., 2018. Detecting, Extracting, and monitoring Surface Water from Space using Optical Sensors: a Review. Rev. Geophys. 56, 333–360. https://doi.org/10.1029/2018RG000598.
Huang, C., Zhang, C., He, Y., Liu, Q., Li, H., Su, F., Liu, G., Bridhikitti, A., 2020. Land Cover Mapping in Cloud-Prone Tropical areas using Sentinel-2 Data: Integrating Spectral Features with Ndvi Temporal Dynamics. Remote Sens. (Basel) 12, 1163. https://doi.org/10.3390/rs12071163.
Karpouzoglou, T., Barron, J., 2014. A global and regional perspective of rainwater harvesting in sub-Saharan Africa's rainfed farming systems. Phys. Chem. Earth, Parts a/b/c 72–75, 43–53. https://doi.org/10.1016/j.pce.2014.09.009.
Keketso, L., 2003. The mixed Blessings of the Lesotho Highlands Water Project: an Assessment based on Local Perspectives. Mt. Res. Dev. 23, 7–10. https://doi.org/10.1659/0276-4741(2003)023[0007:TMBOTL]2.0.CO;2.
Ketchum, D., Hoylman, Z.H., Huntington, J., Brinkerhoff, D., Jencso, K.G., 2023. Irrigation intensification impacts sustainability of streamflow in the Western United States. Commun. Earth Environ. 4, 479. https://doi.org/10.1038/s43247-023-01152-2.
Khalid, H.W., Khalil, R.M.Z., Qureshi, M.A., 2021. Evaluating spectral indices for water bodies extraction in western Tibetan Plateau. Egypt. J. Remote Sens. Space Sci. 24, 619–634. https://doi.org/10.1016/j.ejrs.2021.09.003.
Kotir, J.H., 2011. Climate change and variability in Sub-Saharan Africa: a review of current and future trends and impacts on agriculture and food security. Environ. Dev. Sustain. 13, 587–605. https://doi.org/10.1007/s10668-010-9278-0.
Laonamsai, J., Julphunthong, P., Saprathet, T., Kimmany, B., Ganchanasuragit, T., Chomcheawchan, P., Tomun, N., 2023. Utilizing NDWI, MNDWI, SAVI, WRI, and AWEI for estimating erosion and Deposition in Ping River in Thailand. Hydrology 10, 70. https://doi.org/10.3390/hydrology10030070.
Lehner, B., Grill, G., 2013. Global river hydrography and network routing: baseline data and new approaches to study the world's large river systems. Hydrological Processes 27 (15), 2171–2186. https://doi.org/10.1002/hyp.9740.
Liang, J., Gong, J., Li, W., 2018. Applications and impacts of Google Earth: a decadal review (2006–2016). ISPRS J. Photogramm. Remote Sens. 146, 91–107. https://doi.org/10.1016/j.isprsjprs.2018.08.019.
Li, X., Ling, F., Foody, G.M., Boyd, D.S., Jiang, L., Zhang, Y., Zhou, P., Wang, Y., Chen, R., Du, Y., 2021. Monitoring high spatiotemporal water dynamics by fusing MODIS, Landsat, water occurrence data and DEM. Remote Sens. Environ. 265, 112680. https://doi.org/10.1016/j.rse.2021.112680.
Li, X., Zhang, F., Chan, N.W., Shi, J., Liu, C., Chen, D., 2022. High Precision Extraction of Surface Water from complex Terrain in Bosten Lake Basin based on Water Index and Slope Mask Data. Water 14, 2809. https://doi.org/10.3390/w14182809.
Love, R., 1996. Culture, nationality and dependence: a comparative study of Lesotho. Lesotho Social Sciences Review 2, 1–16.
Lu, S., Wu, B., Yan, N., Wang, H., 2011. Water body mapping method with HJ-1A/B satellite imagery. Int. J. Appl. Earth Obs. Geoinf. 13, 428–434. https://doi.org/10.1016/j.jag.2010.09.006.
Matarira, C.H., Shava, E., Pedzisai, E., Manatsa, D., 2014. Food Insecurity in Mountain Communities of Lesotho. Journal of Hunger & Environmental Nutrition 9, 280–296. https://doi.org/10.1080/19320248.2014.898170.
Maxwell, A.E., Warner, T.A., Fang, F., 2018. Implementation of machine-learning classification in remote sensing: an applied review. Int. J. Remote Sens. 39, 2784–2817. https://doi.org/10.1080/01431161.2018.1433343.
Mbata, J.N., 2001. Land Use Practices in Lesotho: Implications for Sustainability in Agricultural Production. J. Sustain. Agric. 18, 5–24. https://doi.org/10.1300/J064v18n02_03.
McFEETERS, S.K., 1996. The use of the Normalized Difference Water Index (NDWI) in the delineation of open water features. Int. J. Remote Sens. 17, 1425–1432. https://doi.org/10.1080/01431169608948714.
McKight, P.E., Najab, J., 2010. Kruskal-Wallis Test, in: Weiner, I.B., Craighead, W.E. (Eds.), The Corsini Encyclopedia of Psychology. Wiley, pp. 1–1. DOI: 10.1002/9780470479216.corpsy0491.
Moeletsi, M., Walker, S., 2012. Rainy season characteristics of the Free State Province of South Africa with reference to rain-fed maize production. WSA 38, 775–782. https://doi.org/10.4314/wsa.v38i5.17.
Moeti, L., 2007. Irrigation prospects in Lesotho: an Appraisal of the Seaka Irrigation Project. Lesotho Journal of Agricultural Sciences 1 (1), 1–14.
Mohammad, L., Mondal, I., Bandyopadhyay, J., Pham, Q.B., Nguyen, X.C., Dinh, C.D., Al-Quraishi, A.M.F., 2022. Assessment of spatio-temporal trends of satellite-based aerosol optical depth using Mann–Kendall test and Sen's slope estimator model. Geomat. Nat. Haz. Risk 13, 1270–1298. https://doi.org/10.1080/19475705.2022.2070552.
Mohammadi, A., Costelloe, J.F., Ryu, D., 2017. Application of time series of remotely sensed normalized difference water, vegetation and moisture indices in characterizing flood dynamics of large-scale arid zone floodplains. Remote Sens. Environ. 190, 70–82. https://doi.org/10.1016/j.rse.2016.12.003.
Mueller, N., Lewis, A., Roberts, D., Ring, S., Melrose, R., Sixsmith, J., Lymburner, L., McIntyre, A., Tan, P., Curnow, S., Ip, A., 2016. Water observations from space: Mapping surface water from 25 years of Landsat imagery across Australia. Remote Sens. Environ. 174, 341–352. https://doi.org/10.1016/j.rse.2015.11.003.
Mullen, C., Penny, G., Müller, M.F., 2021. A simple cloud-filling approach for remote sensing water cover assessments. Hydrol. Earth Syst. Sci. 25, 2373–2386. https://doi.org/10.5194/hess-25-2373-2021.
Mwangi, O., 2007. Hydropolitics, Ecocide and Human Security in Lesotho: a Case Study of the Lesotho Highlands Water Project *. J. South. Afr. Stud. 33, 3–17. https://doi.org/10.1080/03057070601136509.
Nash, D.J., Grab, S.W., 2010. "A sky of brass and burning winds": documentary evidence of rainfall variability in the Kingdom of Lesotho, Southern Africa, 1824–1900. Clim. Change 101, 617–653. https://doi.org/10.1007/s10584-009-9707-y.
Nyberg, B., Sayre, R., Luijendijk, E., 2024. Increasing seasonal variation in the extent of rivers and lakes from 1984 to 2022. Hydrol. Earth Syst. Sci. 28, 1653–1663. https://doi.org/10.5194/hess-28-1653-2024.
Ogilvie, A., Belaud, G., Massuel, S., Mulligan, M., Le Goulven, P., Calvez, R., 2018. Surface water monitoring in small water bodies: potential and limits of multi-sensor Landsat time series. Hydrol. Earth Syst. Sci. 22, 4349–4380. https://doi.org/10.5194/hess-22-4349-2018.
Pal, M., Mather, P.M., 2005. Support vector machines for classification in remote sensing. Int. J. Remote Sens. 26, 1007–1011. https://doi.org/10.1080/01431160512331314083.
Palazzoli, I., Montanari, A., Ceola, S., 2023. Contribution of anthropogenic and hydroclimatic factors on the variation of surface water extent across the contiguous United States. Environ. Res. Commun. 5, 051006. https://doi.org/10.1088/2515-7620/acd510.
Phuong, D.N.D., Tram, V.N.Q., Nhat, T.T., Ly, T.D., Loi, N.K., 2020. Hydro-meteorological trend analysis using the Mann-Kendall and innovative-şen methodologies: a case study. IJGW 20, 145. https://doi.org/10.1504/IJGW.2020.105385.

Pryor, J.W., Zhang, Q., Arias, M.E., 2022. Integrating climate Change, Hydrology, and Water Footprint to measure Water Scarcity in Lesotho. Africa. J. Water Resour. Plann. Manage. 148, 05021025. https://doi.org/10.1061/(ASCE)WR.1943-5452.0001502.

Ramakhanna, S.J., Mapeshoane, B.E., Omuto, C.T., 2022. Carbon sequestration potential in croplands in Lesotho. Ecol. Model. 471, 110052. https://doi.org/10.1016/j.ecolmodel.2022.110052.

Rantšo, T.A., 2016. The role of infrastructure, markets and government support in the success of small scale enterprises in Lesotho. IJESB 27, 108. https://doi.org/10.1504/IJESB.2016.073360.

R Core Team, R., 2024. R: A language and environment for statistical computing.

Sagan, V., Peterson, K.T., Maimaitijiang, M., Sidike, P., Sloan, J., Greeling, B.A., Maalouf, S., Adams, C., 2020. Monitoring inland water quality using remote sensing: potential and limitations of spectral indices, bio-optical simulations, machine learning, and cloud computing. Earth Sci. Rev. 205, 103187. https://doi.org/10.1016/j.earscirev.2020.103187.

Sawaya, K.E., Olmanson, L.G., Heinert, N.J., Brezonik, P.L., Bauer, M.E., 2003. Extending satellite remote sensing to local scales: land and water resource monitoring using high-resolution imagery. Remote Sens. Environ. 88, 144–156. https://doi.org/10.1016/j.rse.2003.04.006.

Schultz, B.B., 1985. Levene's Test for Relative Variation. Syst. Biol. 34, 449–456. https://doi.org/10.1093/sysbio/34.4.449.

Secu, C.V., Stoleriu, C.C., Lesenciuc, C.D., Ursu, A., 2022. Normalized Sand Index for Identification of Bare Sand areas in Temperate Climates using Landsat Images, Application to the South of Romania. Remote Sens. (Basel) 14, 3802. https://doi.org/10.3390/rs14153802.

Sekamane, T., Nel, W.A.J., McKay, T.J., Tantoh, H.B., 2023. Community perceptions of the social impacts of the Metolong Dam and Reservoir in Lesotho. Land Use Policy 125, 106495. https://doi.org/10.1016/j.landusepol.2022.106495.

Sene, K.J., Jones, D.A., Meigh, J.R., Farquharson, F.A.K., 1998. Rainfall and flow variations in the Lesotho Highlands. Int. J. Climatol. 18, 329–345. https://doi.org/10.1002/(SICI)1097-0088(19980315)18:3<329::AID-JOC251>3.0.CO;2-5.

Serrano, J., Shahidian, S., Marques Da Silva, J., 2019. Evaluation of Normalized Difference Water Index as a Tool for monitoring Pasture Seasonal and Inter-Annual Variability in a Mediterranean Agro-Silvo-Pastoral System. Water 11, 62. https://doi.org/10.3390/w11010062.

Sheffield, J., Wood, E.F., Pan, M., Beck, H., Coccia, G., Serrat-Capdevila, A., Verbist, K., 2018. Satellite Remote Sensing for Water Resources Management: potential for supporting Sustainable Development in Data-Poor Regions. Water Resour. Res. 54, 9724–9758. https://doi.org/10.1029/2017WR022437.

Shen, L., Li, C., 2010. Water body extraction from Landsat ETM+ imagery using adaboost algorithm. In: Presented at the 2010 18th International Conference on Geoinformatics, pp. 1–4.

Sigopi, M., Shoko, C., Dube, T., 2024. Advancements in remote sensing technologies for accurate monitoring and management of surface water resources in Africa: an overview, limitations, and future directions. Geocarto Int. 39, 2347935. https://doi.org/10.1080/10106049.2024.2347935.

Sit, M., Demiray, B.Z., Xiang, Z., Ewing, G.J., Sermet, Y., Demir, I., 2020. A comprehensive review of deep learning applications in hydrology and water resources. Water Sci. Technol. 82, 2635–2670. https://doi.org/10.2166/wst.2020.369.

Soti, V., Tran, A., Bailly, J.-S., Puech, C., Seen, D.L., Bégué, A., 2009. Assessing optical earth observation systems for mapping and monitoring temporary ponds in arid areas. Int. J. Appl. Earth Obs. Geoinf. 11, 344–351. https://doi.org/10.1016/j.jag.2009.05.005.

Stevens, J., Ntai, P., 2011. The role of extension support to irrigation farmers in Lesotho. South African Journal of Agricultural Extension 9 (2), 104–112. https://www.scielo.org.za/scielo.php?script=sci_arttext&pid=S0301-603X2011000200009.

Sun, D., Gao, G., Huang, L., Liu, Y., Liu, D., 2024. Extraction of water bodies from high-resolution remote sensing imagery based on a deep semantic segmentation network. Sci. Rep. 14, 14604. https://doi.org/10.1038/s41598-024-65430-5.

Tesfaye, M., Breuer, L., 2024. Performance of water indices for large-scale water resources monitoring using Sentinel-2 data in Ethiopia. Environ. Monit. Assess. 196, 467. https://doi.org/10.1007/s10661-024-12630-1.

Thorslund, J., Van Vliet, M.T.H., 2020. A global dataset of surface water and groundwater salinity measurements from 1980–2019. Sci. Data 7, 231. https://doi.org/10.1038/s41597-020-0562-z.

Turpie, J., Benn, G., Thompson, M., Barker, N., 2021. Accounting for land cover changes and degradation in the Katse and Mohale Dam catchments of the Lesotho highlands. Afr. J. Range Forage Sci. 38, 53–66. https://doi.org/10.2989/10220119.2020.1846214.

Twisa, S., Buchroithner, M.F., 2019. Seasonal and Annual Rainfall Variability and their Impact on Rural Water Supply Services in the Wami River Basin. Tanzania. Water 11, 2055. https://doi.org/10.3390/w11102055.

Verdin, J.P., 1996. Remote sensing of ephemeral water bodies in western Niger. Int. J. Remote Sens. 17, 733–748. https://doi.org/10.1080/01431169608949041.

Verschuur, J., Li, S., Wolski, P., Otto, F.E.L., 2021. Climate change as a driver of food insecurity in the 2007 Lesotho-South Africa drought. Sci. Rep. 11, 3852. https://doi.org/10.1038/s41598-021-83375-x.

Wang, C., Jiang, W., Deng, Y., Ling, Z., Deng, Y., 2022. Long Time Series Water Extent Analysis for SDG 6.6.1 based on the GEE Platform: a Case Study of Dongting Lake. IEEE J. Sel. Top. Appl. Earth Observations Remote Sensing 15, 490–503. https://doi.org/10.1109/JSTARS.2021.3088127.

Wang, W., Teng, H., Zhao, L., Han, L., 2023. Long-Term changes in Water Body Area Dynamic and Driving Factors in the Middle-lower Yangtze Plain based on Multi-Source Remote Sensing Data. Remote Sens. (Basel) 15, 1816. https://doi.org/10.3390/rs15071816.

Wen, Z., Zhang, C., Shao, G., Wu, S., Atkinson, P.M., 2021. Ensembles of multiple spectral water indices for improving surface water classification. Int. J. Appl. Earth Obs. Geoinf. 96, 102278. https://doi.org/10.1016/j.jag.2020.102278.

Xie, C., Huang, X., Zeng, W., Fang, X., 2016. A novel water index for urban high-resolution eight-band WorldView-2 imagery. Int. J. Digital Earth 9, 925–941. https://doi.org/10.1080/17538947.2016.1170215.

Xu, H., 2006. Modification of normalised difference water index (NDWI) to enhance open water features in remotely sensed imagery. Int. J. Remote Sens. 27, 3025–3033. https://doi.org/10.1080/01431160600589179.

Zanaga, D., Van De Kerchove, R., Daems, D., De Keersmaecker, W., Brockmann, C., Kirches, G., Wevers, J., Cartus, O., Santoro, M., Fritz, S., Lesiv, M., Herold, M., Tsendbazar, N.-E., Xu, P., Ramoino, F., Arino, O., 2022. ESA WorldCover 10 m 2021 v200. DOI: 10.5281/ZENODO.7254221.

Zaremehrjardy, M., Victor, J., Park, S., Smerdon, B., Alessi, D.S., Faramarzi, M., 2022. Assessment of snowmelt and groundwater-surface water dynamics in mountains, foothills, and plains regions in northern latitudes. J. Hydrol. 606, 127449. https://doi.org/10.1016/j.jhydrol.2022.127449.

Zhou, Y., Dong, J., Xiao, X., Xiao, T., Yang, Z., Zhao, G., Zou, Z., Qin, Y., 2017. Open Surface Water Mapping Algorithms: a Comparison of Water-Related Spectral Indices and Sensors. Water 9, 256. https://doi.org/10.3390/w9040256.

Zou, Z., Xiao, X., Dong, J., Qin, Y., Doughty, R.B., Menarguez, M.A., Zhang, G., Wang, J., 2018. Divergent trends of open-surface water body area in the contiguous United States from 1984 to 2016. Proc. Natl. Acad. Sci. U.S.A. 115, 3810–3815. https://doi.org/10.1073/pnas.1719275115.